Estuaries and Coasts (2025) 48:51
https://doi.org/10.1007/s12237-024-01474-0

Biogeochemical and Physical Controls on the Microbial Degradation of Dissolved Organic Matter Along a Temperate Microtidal Estuary

Derek J. Detweiler[1] · Iris C. Anderson[1] · Mark J. Brush[1] · Elizabeth A. Canuel[1]

Received: 11 March 2024 / Revised: 20 November 2024 / Accepted: 2 December 2024 / Published online: 21 January 2025

Abstract

Dissolved organic matter (DOM) is the foundation of the microbial loop and plays an important role in estuarine water quality and ecosystem metabolism. Because estuaries are influenced by DOM with different sources and composition, changing hydrologic regimes, and diverse microbial community assemblages, the biological fate of DOM (i.e., microbial degradation) differs across spatiotemporal scales and between DOM pools. To better understand controls on DOM degradation, we characterized the biogeochemical and physical conditions of the York River Estuary (YRE), a sub-estuary of the Chesapeake Bay in southeast Virginia (USA), during October 2018 and February, April, and July 2019. We then evaluated how these conditions influenced the degradation of dissolved organic carbon (DOC) and nitrogen (DON) and chromophoric dissolved organic matter (CDOM) by conducting parallel dark incubations of surface water collected along the YRE. Compared to other sampling dates, DOC reactivity (ΔDOC (%)) was over two-fold higher in October when freshwater discharge was lower, temperatures were warmer, and autochthonous, aquatic sources of DOC dominated. ΔDOC (%) was near zero when allochthonous, terrestrial sources of DOC were more abundant and when temperatures were cooler during higher discharge periods in February when precipitation in the Chesapeake Bay region was anomalously high. DON was up to six times less reactive than DOC and was sometimes produced during the incubations whereas ΔCDOM (%) was highly variable between sampling periods. Like ΔDOC (%), spatiotemporal patterns in ΔDON (%) were controlled primarily by hydrology and DOM source and composition. Our results show that higher freshwater discharge associated with prolonged wet periods decreased estuarine flushing time and increased the delivery of allochthonous DOM derived from terrestrial sources into coastal waters, resulting in lower rates of DOM degradation especially under cool conditions. While these findings provide evidence for seasonal variation in DOM degradation, shifting environmental conditions (e.g., increasing temperatures and precipitation) due to climate change may also have interactive effects on the magnitude and composition of DOM exported to estuaries and its subsequent reactivity.

Keywords Carbon · Nitrogen · CDOM · Estuary · Organic matter · Decomposition

Introduction

Estuaries are "hotspots" of organic matter (OM) cycling and play an important role in the coastal carbon cycle due to their position at the land-sea interface (McClain et al. 2003). This location is characterized by both allochthonous (i.e., produced outside the estuary) inputs of OM from rivers and the surrounding catchments and autochthonous (i.e., produced within the estuary) inputs of OM from primary and secondary production. During transport to the coastal ocean, allochthonous and autochthonous sources of OM may be modified and removed by processes such as flocculation, sinking, photolysis, and microbial degradation (Canuel and Hardison 2016; Bianchi 2007 and references therein; Hedges and Keil 1999). Understanding the effect of these processes on OM is important for determining the trophic status of estuaries, developing coastal carbon budgets, and assessing the role of estuaries as either sources or sinks of carbon dioxide (CO_2) (Borges and Abril 2011; Cai 2011).

Dissolved organic carbon (DOC) comprises most of the total dissolved organic matter (DOM) pool, but DOM also

Communicated by Xuefeng Peng

✉ Derek J. Detweiler
djdetweiler@vims.edu

[1] Virginia Institute of Marine Science, William & Mary, P.O. Box 1346, Gloucester Point, VA 23062, USA

includes other constituents such as dissolved organic nitrogen (DON), dissolved organic phosphorus (DOP), and dissolved organic sulfur (DOS) (Bianchi 2007 and references therein). In addition, chromophoric dissolved organic matter (CDOM) is a component of DOM that absorbs light. Within CDOM, there is a fraction that fluoresces (i.e., fluorescent dissolved organic matter or fDOM). Optical properties (absorbance and fluorescence) of DOM are often used to identify the source and composition of DOM in estuaries and other aquatic ecosystems (Stedmon and Nelson 2015). DOC dynamics are often used to describe the entire DOM pool (Carlson and Hansell 2015), but DOM components may have different fates depending on the relative contributions of each to the total DOM pool (e.g., elemental stoichiometry) and their interactions with biotic and abiotic environmental factors (Graeber et al. 2021; Asmala et al. 2013; Lønberg et al. 2010).

Microbial degradation represents an important fate of DOM in estuaries and is influenced by chemical (e.g., source and composition), physical (e.g., temperature, freshwater discharge), and biological (e.g., microbial community) factors (McCallister et al. 2006; Smith and Benner 2005; Hopkinson et al. 1998). For example, terrestrial DOM (e.g., humic material) is mainly derived from soil and vascular plants and is characterized by macromolecules that are highly aromatic, polymerized, and function as structural components (Zark and Dittmar 2018; Bianchi 2011). In comparison, aquatic DOM (e.g., proteins, amino and nucleic acids) is primarily derived from microbial sources and is composed of N-rich biomolecules (Sleighter and Hatcher 2008; Holmer 1996; Bronk and Gilbert 1993). Therefore, aquatic DOM tends to have higher nutritional value and requires less energy for degradation compared to terrestrial DOM (He et al. 2020; Bauer and Bianchi 2011). The microbial degradation of DOM can be enhanced under favorable environmental and biological conditions (e.g., in the presence of oxygen, light, or specific microbial taxa) (Medeiros et al. 2015; Bianchi 2011; McCallister et al. 2005; Miller and Moran 1997). For example, terrestrial DOM mobilized and delivered to an estuary during high discharge events can be susceptible to high rates of bacterial and photochemical degradation due to light and oxygen exposure (Letourneau et al. 2021; Osburn et al. 2019). Extreme freshwater discharge, however, also reduces water residence and processing time, which can limit the degradation of DOM until it reaches the coastal ocean (Hounshell et al. 2019). In addition, the timescale at which terrestrial DOM is delivered to and degraded within estuaries varies and depends on features of the study system such as flushing time and overall geography and geomorphology (Bukaveckas 2022; Raymond et al. 2016; Spencer et al. 2008).

To improve understanding of microbial degradation of DOM in estuaries, we characterized physical (e.g., hydrology) and biogeochemical (e.g., DOM source and composition, nutrients) conditions of the York River estuary (YRE), a sub-estuary of the Chesapeake Bay in southeast Virginia (USA) and representative of temperate, microtidal systems common along the east coast of the USA. We then evaluated how these conditions influenced DOC, DON, and CDOM reactivity by conducting parallel dark laboratory incubation experiments of surface water collected seasonally along the YRE salinity gradient.

Overall, we hypothesized that rates of DOM degradation would be higher when autochthonous, aquatic sources of DOM were more abundant in the estuary whereas rates of degradation would be lower when allochthonous, terrestrial sources of DOM dominated. We also expected that freshwater discharge and flushing time would be predictors of DOM reactivity because of their effects on the sources and composition of DOM.

Methods

Site Description

A detailed description of the YRE and surrounding watershed can be found in Reay (2009), Reay and Moore (2009), and Friedrichs (2009). Briefly, the YRE is a temperate microtidal sub-estuary of the Chesapeake Bay in southeast Virginia (USA). The Pamunkey and Mattaponi Rivers, two major tributaries of the YRE, converge 52 km from the mouth of the Chesapeake Bay near West Point, VA. These two tributaries are responsible for most freshwater discharge to the YRE with a combined mean streamflow of 4.06×10^6 m^3 d^{-1}. The YRE has a mean tidal range of 0.70–0.85 m, and the surrounding watershed is ~ 60% forested and undeveloped with pockets of agriculture (~ 20%) and residential and commercial development (~ 2%). Tidal wetlands comprise ~ 7% of the watershed including freshwater marshes in the Pamunkey and Mattaponi Rivers as well as salt marshes along the mainstem York River. Mean salinity ranges from 0 at the uppermost reaches of the Pamunkey and Mattaponi Rivers to 20 at the mouth of the York River.

Sample Collection and Physical and Biogeochemical Conditions of the YRE

During October 2018 and February, April, and July 2019, triplicate surface water samples (< 0.5 m below the surface) were collected from three locations along the YRE estuarine salinity gradient, hereafter referred to as upper (37° 28′ 48.4″ N 76° 45′ 34.2″ W), middle (37° 20′ 13.2″ N 76° 38′ 24.0″ W), and lower (37° 15′ 06.5″ N 76° 26′ 34.4″ W) (Fig. 1). Samples were collected using a DataFlow pump intake system (see Crosswell et al. 2017). A tidal freshwater site on

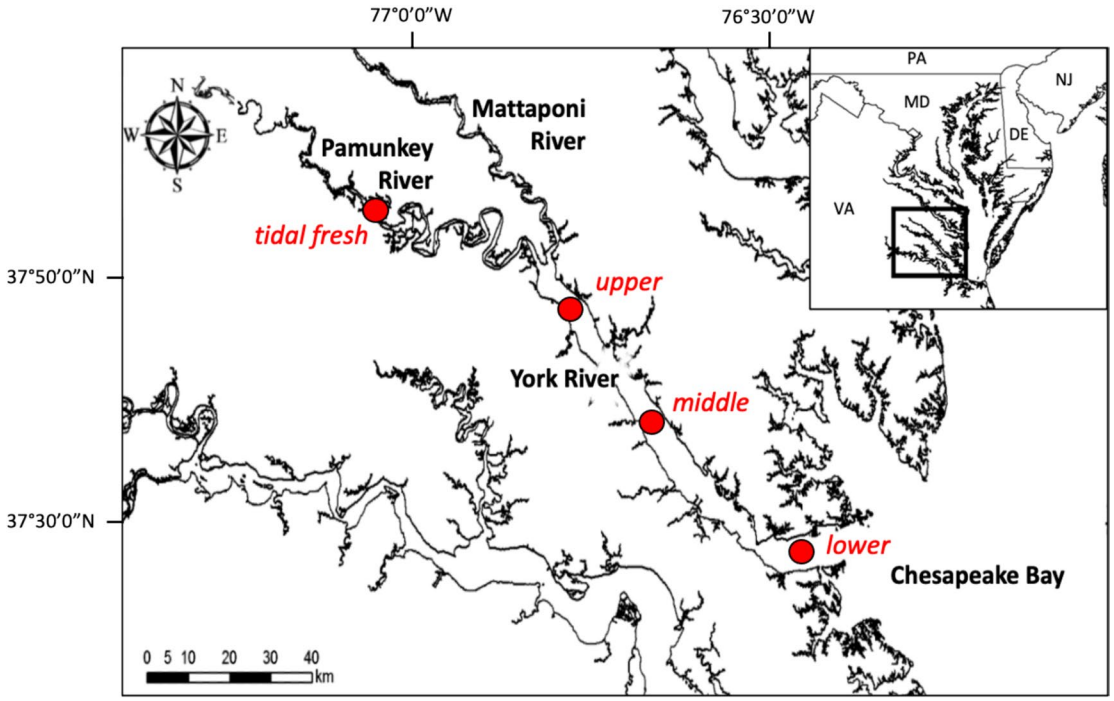

Fig. 1 Sampling locations (red dots) along the YRE. Three locations (upper, middle, lower) along the mainstem York River were sampled in October 2018 and February, April, and July 2019. One location in the tidal freshwater portion of the Pamunkey River was only sampled in October 2018 and February 2019

the Pamunkey River (37° 34′ 17.0″ N 76° 53′ 02.3″ W) was sampled in October 2018 and February 2019 (Fig. 1). Surface water samples were dispensed directly into 2L polycarbonate bottles and kept in the dark on ice for transport back to the Virginia Institute of Marine Science (VIMS). Prior to sample collection, all glassware and glass-fiber filters were combusted (500 °C for 4 h), and polyethersulfone (PES) filters and polycarbonate collection bottles were acid-rinsed (10% HCl).

Concurrent single-point measurements of temperature, salinity, pH, and dissolved oxygen (DO) were made using a multi-parameter data sonde (YSI 6600V2). Additional water column samples were collected to assess in situ concentrations of dissolved inorganic carbon (DIC) (Neubauer and Anderson 2003), dissolved inorganic nitrogen (DIN) as ammonium (NH_4^+) and nitrite + nitrate (NO_x) (Liao 2001; Smith and Bogren 2001; Koroleff 1983), chlorophyll-*a* (Anderson et al. 2003), and absorbance of CDOM at 440 nm (a_{440}) normalized to DOC concentration (a^*_{440}) (Pucher et al. 2019; Tzortziou et al. 2008). DIC measurements had a 2 µM detection limit and ~ 2 µM precision across sample injections. NH_4^+ measurements had a 0.1 µM detection limit and ~ 0.1 µM precision across sample injections, and NO_x measurements had a 0.05 µM detection limit and ~ 0.1 µM precision across sample injections.

Freshwater discharge data were obtained from the United States Geological Survey (USGS) National Water Information System for the Pamunkey (USGS 01673000) and Mattaponi (USGS 01674500) Rivers (https://waterdata.usgs.gov/nwis/). Flushing time (FT), defined as the amount of time it takes to replace existing freshwater in an estuary, was calculated using a salt balance approach (Officer 1980) within an existing box model of the YRE (Lake and Brush 2015) which computes exchanges and FT as functions of salinity and freshwater inputs in eight boxes, one each in the lower Pamunkey and Mattaponi Rivers, and six down the main axis of the YRE. The average FT for a given box along the axis of the estuary is given by the following:

$$FT_m = \frac{(s_m - s_{m-1})(s_{m+1} - s_m)}{s_m(s_{m+1} - s_{m-1})} \times \frac{V_m}{R}$$

where s is salinity, m is any given box along the estuary, V is box volume (m^3), and R is freshwater discharge ($m^3\ d^{-1}$). The subscripts $m-1$ and $m+1$ represent boxes upstream and downstream of box m, respectively. FT was computed in each box along the axis of the estuary and then used to estimate the approximate freshwater age (FW age), defined as the approximate age (in days) of the freshwater in a given box along the estuary (i.e., time since entering the system), following:

$$FWage_m = \overline{FT_{\text{Pamunkey}} + FT_{\text{Mattaponi}}} + \left(FT_{m-1} + FT_{m-2} \ldots\right) + (FT_m/2)$$

where $\overline{FT_{\text{Pamunkey}} + FT_{\text{Mattaponi}}}$ corresponds to the average FT in the lower Pamunkey and Mattaponi boxes, $\left(FT_{m-1} + FT_{m-2} \ldots\right)$ corresponds to the sum of FT in all other boxes upstream from box m, and FT_m corresponds to the FT of any given box for which the FW age is calculated.

In this study, the bulk FT metric was used instead of residence time, defined as the amount of time it takes a parcel of water to exit an estuary, as it provides an integrative metric for assessing the effects of freshwater discharge on estuarine water flow and material processing (Monsen et al. 2002). The use of FT also allowed us to approximate the age of freshwater along the axis of the estuary; while our calculation of age does not use the formal location-specific, particle tracking approach common to such estimates (e.g., Monsen et al. 2002), it nevertheless provides an integrative proxy of time since the freshwater in each box first entered the estuary.

Microbial Degradation Experiments

Upon return to VIMS, the 2 L water samples were immediately filtered sequentially through 0.7 µm (Whatman GF/F) and 0.2 µm (Sterlitech PES) filters into borosilicate glass bottles. The 0.2 µm filtrate was inoculated with the 0.7 µm filtrate (1% v/v) for microbial degradation experiments following similar studies (Lu et al. 2013; McCallister et al. 2006). The samples were incubated in a controlled environment room (Environmental Growth Chambers, Chagrin Falls, Ohio) under dark and aerobic conditions at in situ York River water temperature averaged along the estuary (25 °C in October, 4 °C in February, 12 °C in April, and 29 °C in July). Bottles were then sub-sampled at the onset of the experiment (T_0), one day following onset (T_1), and weekly for 28 days thereafter (T_7, T_{14}, T_{21}, T_{28}). Uninoculated samples (0.2 µm filtrate only) were also incubated as a control treatment without microbial degradation (DOC and DON only). Dissolved oxygen was monitored for the duration of each incubation to verify that conditions remained aerobic.

Subsamples for DOC and DON were filtered (0.45 µm PES) and frozen (− 20 °C) while those for CDOM were filtered (0.2 µm PES) and refrigerated (4 °C) until analyses were completed within four weeks of collection. A 0.2 µm filter pore size and refrigerated storage were chosen for CDOM samples as best practice for preventing microbial alteration of CDOM components because frozen storage can alter the optical properties of DOM (Chow et al. 2022; Schneider-Zapp et al. 2013).

Concentrations of DOC ([DOC]; µM) at each time point were measured using high-temperature combustion oxidation (Shimadzu TOC-V organic carbon analyzer) with a 0.3 µM detection limit and ~ 0.1 µM precision across sample injections. Microbial degradation was calculated as the percent change in [DOC] between initial (T_0) and final (T_{28}) time points using:

$$\Delta\text{DOC}(\%) = \frac{\left([\text{DOC}]_{\text{final}} - [\text{DOC}]_{\text{initial}}\right)}{[\text{DOC}]_{\text{initial}}} \times 100$$

This standardized measure of reactivity was selected to make direct comparisons with similar microbial degradation studies conducted in the YRE (Lu et al. 2013; McCallister et al. 2006, 2005) and other estuarine systems (Hitchcock and Mitrovic 2015; Wu et al. 2019; Moran et al. 2000) and because of the relative linearity in [ΔDOC] across all time points (Fig. S1).

Concentrations of DON ([DON]; µM) were calculated by subtracting [DIN] (µM) from total dissolved nitrogen ([TDN]; µM) following persulfate digestion (Liao 2001; Smith and Bogren 2001; Koroleff 1983) and colorimetric analysis (Lachat QuikChem 8000 Flow Injection Analysis System). Microbial degradation of DON (ΔDON (%)) was calculated as described above for DOC. DON was not measured during the October 2018 incubations.

DOM Source Characterization

Samples for $\delta^{13}C_{\text{DOC}}$ were collected at the onset of each experiment, filtered (0.45 µm), frozen (− 20 °C), and sent to the North Carolina State University Aquatic Biogeochemistry Laboratory. Stable carbon isotope values are reported in standard δ notation as follows:

$$\delta^{13}C_{\text{DOC}} = \left[\left(\frac{R_{\text{sample}}}{R_{\text{standard}}}\right) - 1\right] \times 10^3$$

where R is $^{13}C/^{12}C$.

DOM composition at each timepoint was determined by measuring absorbance (Shimadzu UV-1800 UV/Vis Scanning Spectrophotometer), fluorescence (Shimadzu RF-6000 spectrofluorophotometer), and resulting excitation-emission matrices (EEMs) of water samples following parameters described in Tzortziou et al. (2008) and Coble (1996). EEMs were compiled and formatted for analyses in the R package staRdom (Pucher et al. 2019). DOM was described as aquatic protein-like or terrestrial humic-like based on peak excitation-emission wavelengths of fDOM as described in Murphy et al. (2013) and Coble (1996). Fluorescent DOM intensities were normalized to standard Raman Units (RU) by dividing all intensities by the area of the Raman peak of an ultrapure water sample (Lawaetz and Stedmon 2009). Protein-like and humic-like CDOM were therefore inferred by fDOM intensities. Lastly, the molecular weight of DOM was estimated using the ratio of the spectral slope within the log-transformed absorption of 275–295 nm and 350–400 nm

(i.e., slope ratio, S_R). A low S_R is indicative of DOM with high molecular weight and has been attributed to allochthonous DOM; a high S_R is indicative of DOM with low molecular weight and has been attributed to autochthonous DOM (Helms et al. 2008).

Changes in protein-like ($\Delta CDOM_{protein\text{-}like}$ (%)) and humic-like ($\Delta CDOM_{humic\text{-}like}$ (%)) CDOM during the incubations were calculated using the approach described above for DOC. These pools are used as indicators of autochthonous aquatic versus allochthonous terrigenous DOM components, respectively (Osburn et al. 2016a; Hudson et al. 2007; Coble 2007). While optical properties of DOM are largely altered by photochemical processes not considered in this study, they are also altered by microbial communities regardless of light conditions (Logozzo et al. 2021; Fasching et al. 2014; Lu et al. 2013; McCallister et al. 2006).

Statistical Analyses

All statistical analyses were performed in R (v4.1.2). Prior to the analyses, all statistical assumptions were assessed using the Shapiro–Wilk test for normality, Levene's test for equality of variances, and Rosner's test for extreme outliers using the R package EnvStats (Millard 2013). Measurements were log-transformed when necessary to meet the assumption for normality. ΔDOC (%), ΔDON (%), and ΔCDOM (%) were compared between sampling dates and locations using the two-way analysis of variance (ANOVA) with interactions followed by Tukey's Honest Significant Difference test for multiple comparisons. Differences were considered significant when $p < 0.05$. ANOVA was used to analyze biogeochemical parameters, $\delta^{13}C_{DOC}$, and absorbance and fluorescence measurements to assess how the initial environmental conditions and DOM source and composition varied between sampling dates and locations.

To determine major drivers of DOC, DON, and CDOM reactivity, multiple linear regression analyses testing all possible subsets of predictor variables were performed. Values for ΔDOC (%), ΔDON (%), and ΔCDOM (%) were removed if they exceeded the threshold resulting from Rosner's test for extreme outliers and if they were not significantly different from zero. Variables were standardized and assessed for collinearity using the variance inflation factor (VIF). The final model was selected by considering the total variance explained by the model (adjusted r^2); the relevance of individual relationships between biogeochemical and physical parameters and ΔDOC (%), ΔDON (%), and ΔCDOM (%); the degree of collinearity between variables; and the corrected Akaike Information Criterion (AICc) (Table S1).

Results

Physical Conditions

Physical variables varied temporally and spatially. Seasonal change in surface water temperature was greatest in the upper estuary (4.55 °C in February to 29.9 °C in July; Table 1). Salinity ranged from 4.10 in the upper estuary in February to 15.8 in the lower estuary in July (Table 1). In general, salinity, pH, and DO increased from the upper to lower estuary across all sampling dates (Table 1). Freshwater age increased from the upper to lower estuary across all sampling dates and encompassed a range of 4.28 days in the upper estuary in April to 47.7 days in the lower estuary in July (Table 1).

Biogeochemical Conditions

There were some spatial and temporal differences in the concentrations of chlorophyll-*a*, DOC, DON, DIC, NO_x, NH_4^+,

Table 1 Physical conditions of the YRE during the study period

Month	Location along estuary	Surface water temperature (°C)	Salinity	pH	Dissolved oxygen (mg L^{-1})	Flushing time (d)	Freshwater age (d)
October	Upper	25.3	5.89	7.27	5.42	3.88	6.43
	Middle	25.6	12.2	7.71	6.25	3.99	14.7
	Lower	26.1	15.0	8.13	6.95	1.22	22.7
February	Upper	4.55	4.10	7.44	11.3	3.21	5.01
	Middle	5.11	8.34	7.87	11.9	3.30	11.8
	Lower	5.27	12.6	8.41	13.4	1.02	18.5
April	Upper	12.0	5.44	7.30	8.34	2.84	4.28
	Middle	12.7	8.95	8.65	10.3	2.93	10.3
	Lower	11.8	12.3	8.61	11.6	0.90	16.2
July	Upper	29.9	9.71	7.16	4.81	7.61	15.8
	Middle	29.7	14.7	7.57	5.45	7.79	32.1
	Lower	29.3	15.8	8.38	7.74	2.33	47.7

ratios of DOC:DON, and CDOM absorbance (Fig. 2; Tables S2-S4). For example, chlorophyll-*a* concentrations pooled across all locations were higher in July than in February ($p = 0.02$; Fig. 2a; Tables S2, S5). Chlorophyll-*a* concentrations were higher in the lower estuary in February and April whereas they were higher in the upper and middle estuary in October and July (Fig. 2a; Tables S2, S5). Particularly high chlorophyll-*a* concentrations were observed in the lower estuary in April (Fig. 2a; Table S2). Initial [DOC] was higher in October compared to all other sampling dates ($p < 0.01$; Fig. 2b; Tables S3, S5). Initial [DON] was higher in July compared to February and April ($p < 0.01$; Fig. 2c; Tables S3, S5). Ratios of DOC:DON were overall lower in July compared to February ($p < 0.01$) and April ($p = 0.03$; Fig. 2d; Tables S2, S5). Ratios of DOC:DON could not be computed for October because DON was not measured. [DIC] pooled across all locations was higher in October and July compared to February and April ($p < 0.01$; Fig. 2e; Tables S2, S5), and [DIC] was consistently lower in the upper estuary compared to both the middle and lower estuary ($p < 0.01$; Fig. 2e; Tables S2, S5). Notable increases in [NO_x] and [NH_4^+] were observed from the upper to lower estuary in February that were not observed during any other time (Fig. 2f and g; Table S2). In April, [NO_x] and [NH_4^+] substantially decreased from the upper to middle estuary (Fig. 2f and g; Table S2).

CDOM absorbance (a_{440}) was overall higher in October compared to February ($p < 0.01$), while absorbance in both October and July was higher than in April ($p < 0.04$; Tables S2, S5). CDOM absorbance also generally decreased from the upper to lower estuary except in February when it increased from the upper to lower estuary (Table S2). CDOM absorbance normalized to DOC concentration (a^*_{440}) did not differ by sampling date but generally decreased from the upper to lower estuary except in February when it increased from the upper to lower estuary (Fig. 2h; Tables S2, S4-S5).

DOM Source Characterization

Mean $\delta^{13}C_{DOC}$ values were higher (more positive) in October and July compared to February (Fig. 2i; Tables S2, S5), and while not statistically significant, $\delta^{13}C_{DOC}$ values generally increased (became more positive) from the upper to lower estuary except in February (Fig. 2i; Table S2). Protein-like CDOM (inferred by fDOM) fluorescence pooled across all locations was higher in October compared to February and April (Fig. 2j; Tables S3, S5). While humic-like CDOM fluorescence did not differ statistically across dates, it was

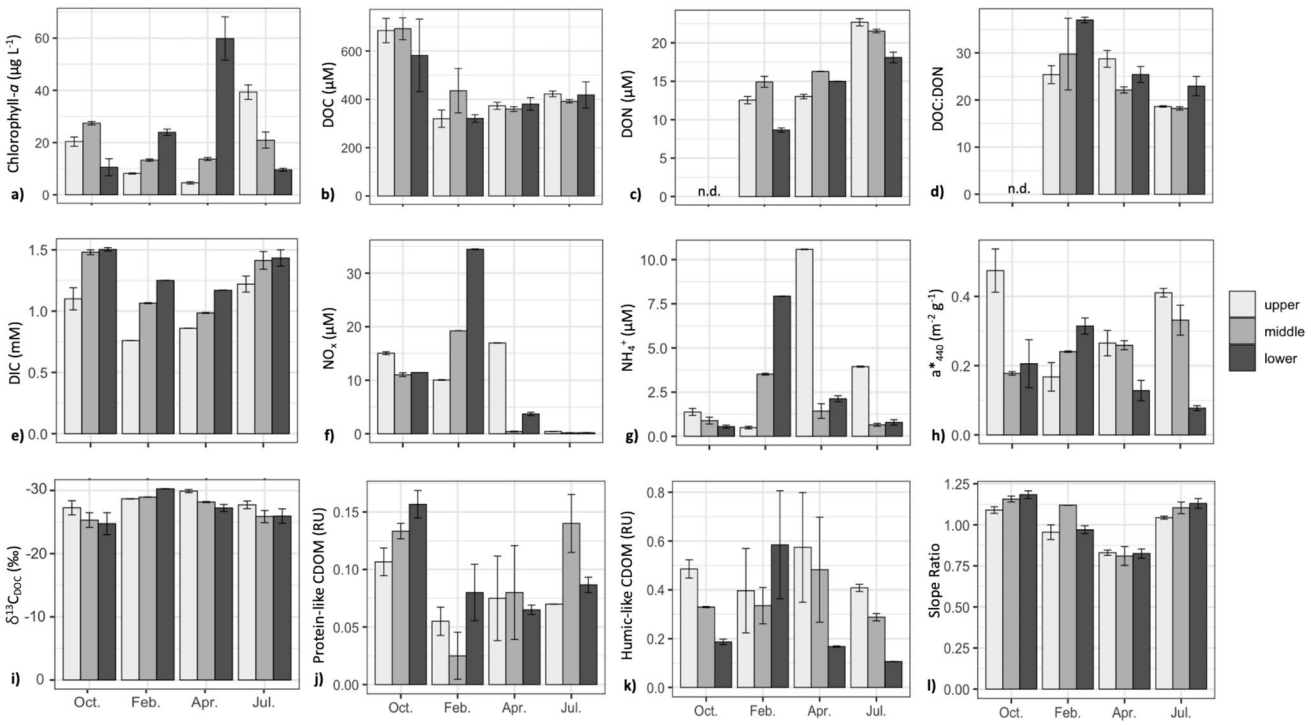

Fig. 2 Initial concentrations and values of biogeochemical variables measured during the study period: **a** chlorophyll-*a*, **b** DOC, **c** DON, **d** DOC:DON, **e** DIC, **f** NO_x, **g** NH_4^+, **h** total CDOM normalized to [DOC] (a^*_{440}), **i** stable isotopes of DOC ($\delta^{13}C_{DOC}$), **j** protein-like CDOM, **k** humic-like CDOM, and **l** slope ratio. Values for each parameter are also presented in Supplementary Tables S2-S3. Error bars are the standard error of the mean of triplicate samples. Refer to text and Supplementary Tables S4-S5 for statistical differences between sampling dates (October, February, April, July) and location along the estuary (upper, middle, lower). n.d., no data

generally higher in the upper and middle estuary (Fig. 2k; Tables S3-S5). Across locations, slope ratio (S_R) was higher in October and July (Fig. 2l; Tables S2, S5). S_R was also higher in February compared to April (Fig. 2l; Tables S2, S5). Although the differences were not statistically significant, S_R increased from the upper to lower estuary in October and July (Fig. 2l; Table S2).

Microbial Degradation of DOM

ΔDOC (%) varied temporally more than spatially (Fig. 3a; Tables S4-S6). A two-way ANOVA revealed differences between sampling dates ($p < 0.01$) but not sampling locations or date × location (Table S4). A higher proportion (up to two-fold) of DOC was lost during the incubations in October (−34 to −41%) compared to February and July (Fig. 3a; Tables S5-S6). Additionally, [DOC] sometimes increased (positive ΔDOC (%) values) at the upper and middle estuary locations during the February incubations; however, the mean values across treatments were not significantly different from zero (Fig. 3a; Table S6).

ΔDON (%) varied temporally and spatially (Fig. 3b; Tables S4-S6). A two-way ANOVA revealed differences in ΔDON (%) between sampling dates ($p < 0.01$), sampling locations ($p < 0.01$), and date × location ($p < 0.01$; Table S4). Interestingly, ΔDON (%) increased during some incubations in April (upper and lower estuary locations) whereas ΔDON (%) decreased at the upper and middle estuary locations in February and at all locations in July (Fig. 3b; Table S6). ΔDON (%) was not measured in October. Mean ΔDON (%) across all sampling dates was also higher in the middle estuary compared to the upper and lower estuary (Fig. 3b; Table S5).

$\Delta CDOM_{protein\text{-}like}$ (%) and $\Delta CDOM_{humic\text{-}like}$ (%) were highly variable during the study period, and there were no clear spatiotemporal trends (Fig. 4; Tables S4-S6). However, a separate ANOVA comparing mean $\Delta CDOM_{protein\text{-}like}$ (%) to mean $\Delta CDOM_{humic\text{-}like}$ (%) across all sampling dates and locations revealed that $\Delta CDOM_{protein\text{-}like}$ (%) was overall more reactive than $\Delta CDOM_{humic\text{-}like}$ (%) excluding incubations when protein-like CDOM was produced (i.e., middle estuary in February and April) ($p < 0.01$; Fig. 4; Table S6).

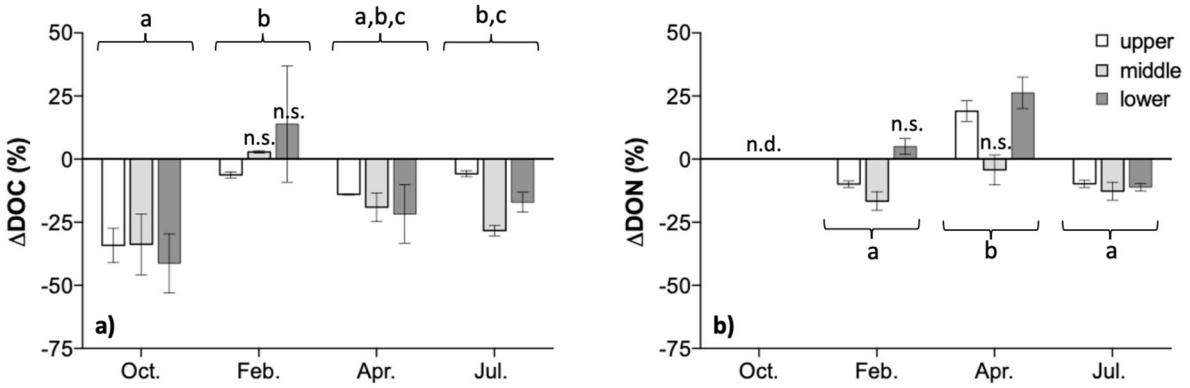

Fig. 3 Mean percent change in the concentration of **a** DOC and **b** DON over 28-day incubation experiments. Samples were collected along the upper, middle, and lower YRE during October 2018 and February, April, and July 2019. Error bars are ± 1 standard error of the mean of triplicate samples. Letters represent statistical comparisons ($p < 0.05$) between seasons. n.d., no data. n.s., ΔDOC (%) or ΔDON (%) was not significantly different from zero

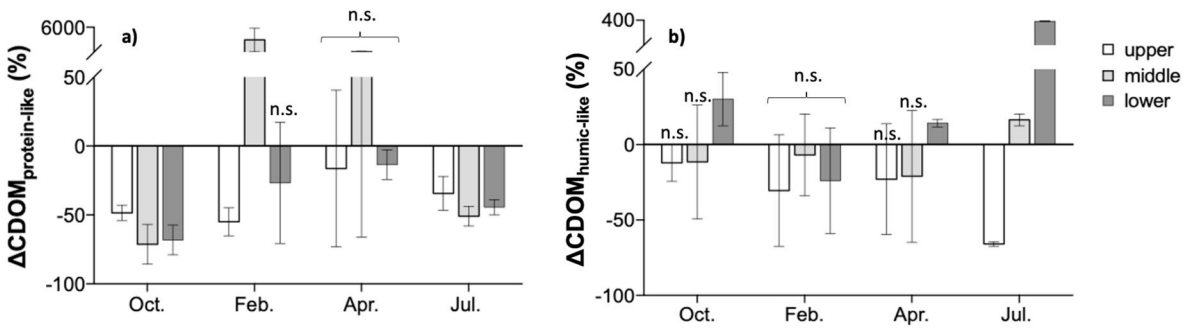

Fig. 4 Mean percent change in **a** protein-like and **b** terrestrial humic-like CDOM over 28-day incubation experiments. Samples were collected along the upper, middle, and lower YRE during October 2018 and February, April, and July 2019. Error bars are ± 1 standard error of the mean of triplicate samples. Note differences in the *y*-axes. n.s., ΔCDOM (%) was not significantly different from zero

Predictors of DOC, DON, and CDOM Degradation

The physical and initial biogeochemical variables (Tables 1, S2-S3) were analyzed as predictors for ΔDOC (%), ΔDON (%), and ΔCDOM (%). Multiple linear regression modeling revealed that ΔDOC (%) was best explained by $\delta^{13}C_{DOC}$, temperature, flushing time, and freshwater age (Table 2). Temperature had the greatest effect on ΔDOC (%) followed by DOC source ($\delta^{13}C_{DOC}$) in the multiple regression model. However, when analyzed as simple regressions, ΔDOC (%) had a stronger linear relationship with $\delta^{13}C_{DOC}$ (adj. $r^2 = 0.37$; $p < 0.01$) compared to temperature (adj. $r^2 = 0.14$; $p = 0.03$) (Fig. 5). Higher (more positive) $\delta^{13}C_{DOC}$ values typical of estuarine phytoplankton were associated with higher ΔDOC (%) while lower $\delta^{13}C_{DOC}$ values typical of terrestrial vascular plants and soils were associated with lower ΔDOC (%). Additionally, warmer temperatures were associated with higher ΔDOC (%). Flushing time and freshwater

Table 2 Multiple linear regression models for predicting DOC and DON degradation as informed by testing all subsets of predictor variables and by resulting corrected Akaike Information Criterion (AICc) values

Predictor	VIF	Estimate (unstandardized)	Std. error (unstandardized)	Estimate (standardized)	Std. error (standardized)	*t*-value	Pr (>|*t*|)
DOC							
Overall model: $F = 8.47$; adj. $r^2 = 0.51$; AICc = 251.2							
$\delta^{13}C_{DOC}$ (‰)	1.77	4.57	1.54	9.88	3.32	2.97	0.006
Temperature (°C)	3.00	1.08	0.44	10.9	4.42	2.47	0.021
Flushing time (d)	1.62	−2.45	1.38	−5.37	3.02	−1.78	0.088
Freshwater age (d)	1.55	−0.62	0.25	−7.47	2.96	−2.53	0.018
DON							
Overall model: $F = 16.49$; adj. $r^2 = 0.86$; AICc = 138.9							
Slope ratio (S_R)	1.77	69.3	12.3	9.21	1.63	5.66	<0.001
Flushing time (d)	4.84	3.92	1.03	8.58	2.25	3.80	0.003
chl-*a* (μg L^{-1})	1.27	−0.31	0.09	−4.86	1.36	−3.58	0.004
[NH_4^+] (μM)	2.01	−1.70	0.52	−5.02	1.54	−3.26	0.007
Protein-like CDOM (RU)	1.81	−177	38.6	−8.02	1.75	−4.58	<0.001
Humic-like CDOM (RU)	1.94	25.1	7.33	5.12	1.50	3.42	0.005
pH	4.04	9.63	4.30	5.09	2.27	2.24	0.045
[DOC] (μM)	1.23	−0.04	0.02	−6.58	3.30	−2.00	0.069

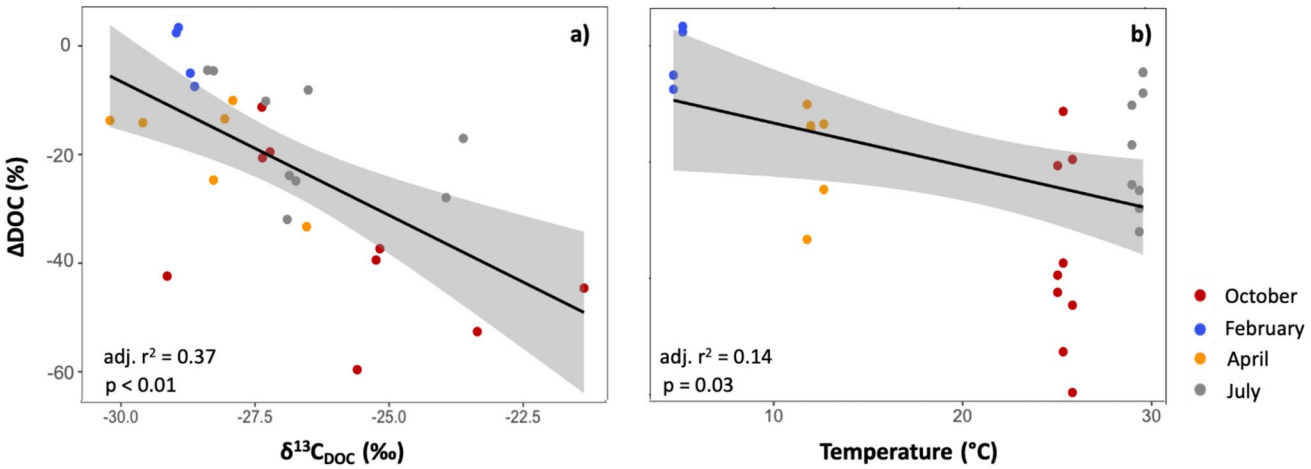

Fig. 5 Bivariate linear regression of **a** stable isotope values of DOC (*x*-axis) and percent change in DOC (*y*-axis) and of **b** water temperature (*x*-axis) and percent change in DOC (*y*-axis). Colors represent samples collected during October 2018 and February, April, and July 2019 pooled across all sampling locations along the YRE. The gray shaded area represents the 95% confidence interval. Values for ΔDOC (%) were removed if they exceeded the threshold resulting from Rosner's test for extreme outliers and if they were not significantly different from zero

age were also predictors of ΔDOC (%) (Table 2), and there was a positive linear relationship between freshwater age and $\delta^{13}C_{DOC}$ (adj. $r^2 = 0.15$; $p < 0.01$) (Fig. 6).

Multiple linear regression modeling revealed that ΔDON (%) was best explained by slope ratio (S_R), flushing time, pH, protein-like and humic-like CDOM, and concentrations of chlorophyll-*a*, NH_4^+, and DOC (Table 2). However, ΔDON (%) had positive linear relationships primarily with S_R (adj. $r^2 = 0.68$; $p < 0.01$) and flushing time (adj. $r^2 = 0.24$; $p = 0.02$) (Fig. 7). DON loss (most negative ΔDON (%)) was greatest when S_R values were highest (i.e., lower molecular weight DOM, autochthonous source) whereas incubations with little DON loss (or DON production) had lower S_R (i.e., higher molecular weight DOM, allochthonous source). In addition, DON loss was greatest when flushing times were longer (Fig. 7).

Because ΔCDOM (%) was highly variable and there were limited instances when ΔCDOM (%) was significantly different from zero (Fig. 4; Table S6), ΔCDOM (%) could not be reliably explained by any of the measured predictors or incorporated into a multiple linear regression analysis.

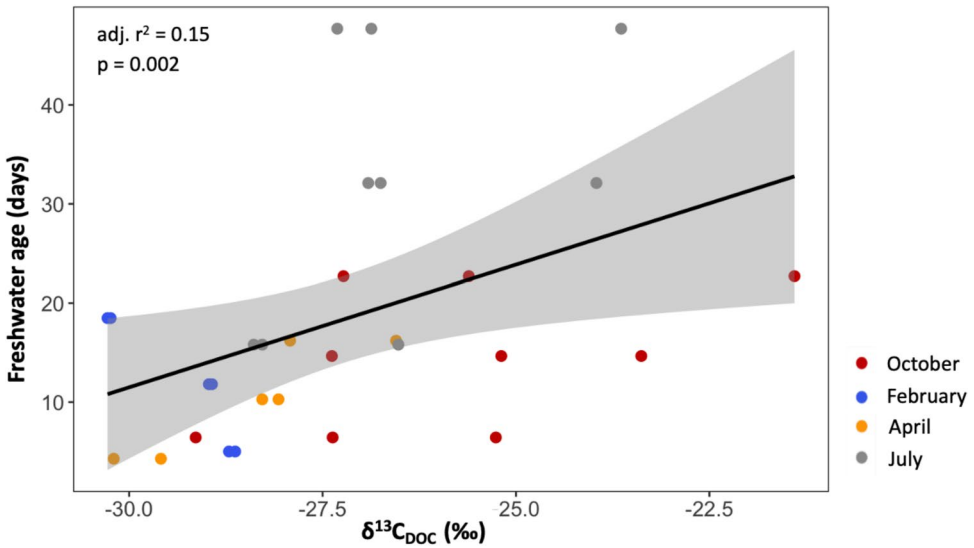

Fig. 6 Bivariate linear regression of stable isotope values of DOC (*x*-axis) and freshwater age (*y*-axis). Colors represent samples collected during October 2018 and February, April, and July 2019 pooled across all sampling locations along the YRE. The gray shaded area represents the 95% confidence interval

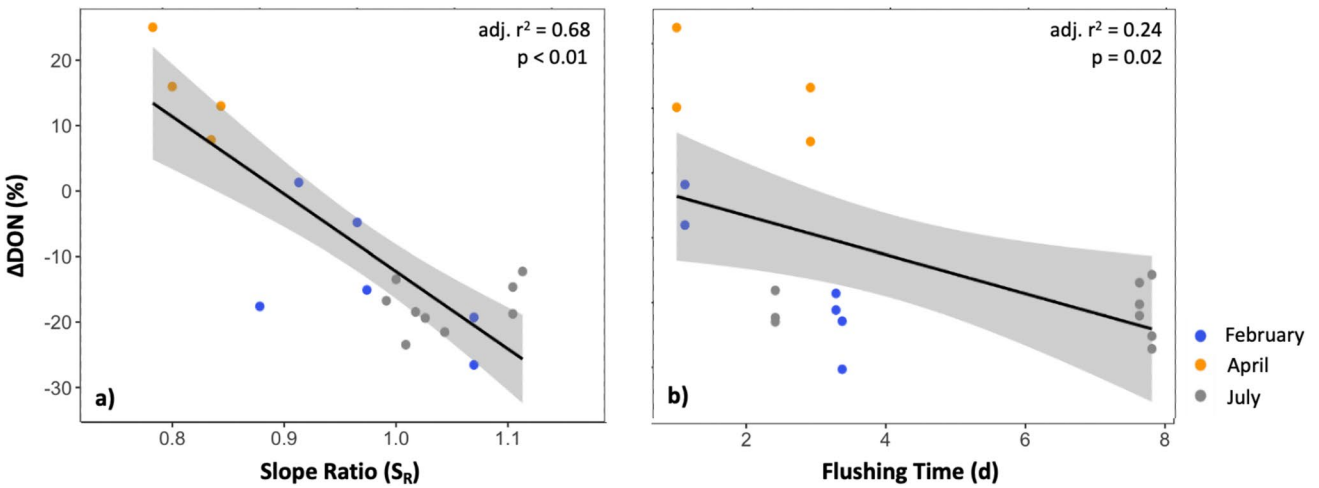

Fig. 7 Bivariate linear regression of **a** slope ratio (*x*-axis) and percent change in DON (*y*-axis) and of **b** flushing time (*x*-axis) and percent change in DON (*y*-axis). Colors represent samples collected during February, April, and July 2019 pooled across all sampling locations along the YRE. DON samples were not collected in October 2018. The gray shaded area represents the 95% confidence interval. Values for ΔDON (%) were removed if they exceeded the threshold resulting from Rosner's test for extreme outliers and if they were not significantly different from zero

Discussion

Physical Conditions of the YRE

Anomalously high freshwater discharge impacted the entire Chesapeake Bay region throughout 2018 and 2019 (Frankel et al. 2022; Chesapeake Bay Foundation 2020). In the YRE, freshwater discharge from the Pamunkey and Mattaponi Rivers was above average, resulting in depressed salinities that deviated from the near-50-year long-term average (1972–2017; Fig. S2). This was especially true in February 2019 when discharge was more than twice the average, resulting in short flushing times and lower freshwater ages approximately one-third of normal conditions that carried into the April 2019 sampling period (Table 1). Overall, these physical conditions along the YRE influenced estuarine biogeochemistry, DOM source and composition, and subsequent DOM degradation as discussed below.

Biogeochemical Conditions of the YRE

High freshwater discharge affected biogeochemical conditions in the YRE. Under normal conditions (e.g., no prolonged wet periods, no phytoplankton blooms), concentrations of biogeochemical constituents are typically highest in the upper estuary (e.g., DON, DIN, DOC) or peak between mid- to lower estuary (e.g., chlorophyll-*a*) depending on residence time and light and nutrient availability (Yao et al. 2019; Countway et al. 2007; McCallister et al. 2006; Bianchi 2007). During the highest discharge period in February, however, concentrations of chlorophyll-*a*, NO_x, and NH_4^+ were highest in the lower estuary, suggesting a potentially rapid down-estuary pulse of nutrients and organic matter (Raymond et al. 2016).

We observed a substantial decrease in NO_x (from ~ 17 to ~ 0.43 µM) and NH_4^+ (from ~ 11 to ~ 1.4 µM) concentrations from the upper to middle estuary in April that coincided with an intense spring phytoplankton bloom of the dinoflagellate *Heterocapsa triquetra.* High discharge in February and April may have affected the persistence of this bloom because 1 week prior to our April 2019 experiment, ~ 35,000 *H. triquetra* cells mL^{-1} were measured in the mid-YRE (Reece, unpub. data). Four days following our study, however, no *H. triquetra* cells were detected in the mid-YRE even though these blooms are known to persist for several weeks (Mulholland 2021; Litaker et al. 2002). Because chlorophyll-*a* can be a strong indicator of phytoplankton abundance (Jakobsen and Markager 2016) including *H. triquetra* (Lindholm and Nummelin 1999), the elevated concentrations of chlorophyll-*a* observed down-estuary (~ 60 µg L^{-1}) suggest that this bloom was quickly flushed towards the mouth of the YRE.

Concentrations of DOC (~ 300–700 µM) and DON (~ 8–23 µM) were generally consistent with previous studies in the YRE, where values ranged from 220 to 518 µM and 15 to 30 µM, respectively (McCallister et al. 2006, 2005; Raymond and Bauer 2001). DOC:DON (~ 18–37) and DIC (0.76–1.51 mM) measurements were also generally consistent with previous studies in the YRE, where values range from 13 to 22 and 0.26 to 1.90 mM, respectively (McCallister et al. 2005; Raymond and Bauer 2001; Raymond et al. 2000). While DOC:DON did not vary spatially, higher ratios in February and April (~ 22–37) compared to July (~ 18–23) are generally consistent with contributions of terrestrial and aquatic sources of OM, respectively (Bianchi 2007; Cloern et al. 2002). DIC concentrations increased from the upper to lower estuary and were higher when freshwater inputs were lower in October and July. These findings are consistent with a previous study that showed increased net heterotrophy down-estuary and increased concentrations of DIC during lower flow periods (Raymond et al. 2000).

DOM Source and Composition

Similar to previous studies, the stable carbon isotope values indicate that the YRE is characterized by a mixture of sources and receives greater inputs of DOM from terrestrial sources during times of higher freshwater discharge (McCallister et al. 2006; Countway et al. 2007). This is evidenced by lower (more negative) $\delta^{13}C_{DOC}$ values, typical of terrestrial plants and soils, in the upper estuary and lower $\delta^{13}C_{DOC}$ values during February and April when freshwater discharge was highest. In contrast, more positive $\delta^{13}C_{DOC}$ values down-estuary (except in February) are indicative of aquatic, microalgal sources and consistent with previous studies showing that primary production is higher in the mid- and lower regions of the YRE (Kim et al. 2021; Lake et al. 2013; Sin et al. 1999) and other estuaries (Andersson et al. 2018; Cloern et al. 2014 and references therein).

We used CDOM characteristics as another proxy for DOM source and composition because $\delta^{13}C_{DOC}$ values for OM sources in estuaries can overlap (Cloern et al. 2002; Sigleo and Macko 1985; Fry and Sherr 1984). CDOM has previously been used to predict DOM concentration, composition, and behavior (Fichot and Benner 2012; Spencer et al. 2007; Del Vecchio and Blough 2004). In the YRE watershed, $\delta^{13}C_{DOC}$ and CDOM characteristics have been successfully coupled to discriminate between source and composition of DOM (Knobloch et al. 2022; Lu et al. 2013). Like these prior studies, our data show that spatiotemporal patterns in humic-like and protein-like CDOM were similar to patterns in the $\delta^{13}C_{DOC}$ values for terrestrial and aquatic sources of DOC, respectively. That is, humic-like CDOM derived from terrestrial sources was higher in the upper

estuary, and less protein-like CDOM derived from aquatic sources was measured in February and April when freshwater delivery was highest (Fig. 2j and k; Table S3).

DOC Degradation

Changes in [DOC] during the incubations ranged from approximately + 14 ± 23 to − 22 ± 12% in February and April and from − 6 ± 1 to − 41 ± 12% in October and July (Fig. 3a; Table S6). Results from October and July fall above the range reported for other estuaries including the Satilla River Estuary, GA (ΔDOC = − 3 to − 9%; Moran et al. 2000); San Francisco Estuary, CA (ΔDOC = − 11 to − 15%; Sobczak et al. 2002); Cape Fear River Estuary, NC (ΔDOC = − 1 to 14%; Avery et al. 2003); Altamaha River Estuary, GA (ΔDOC = − 9 to − 12%; Martineac et al. 2021); and several southeast Texas estuaries (ΔDOC = 0 to −11%; Wu et al. 2019) (Table 3). Results from October and July also fall above the range reported previously for DOC reactivity in the YRE where sampling locations, experimental design, sample processing, and data analyses were similar to the methods used in this study (Table 3). Prior studies in the headwaters of the YRE reported ΔDOC ranging from 0 to − 24% (Lu et al. 2013) while studies along the YRE reported ΔDOC ranging from − 4 to − 19% (McCallister et al. 2006, 2005; Raymond and Bauer 2001). Compared to these studies, our study covered a wider range of environmental conditions and incubation temperatures. Additionally, the YRE watershed experienced an 8% increase in land development (e.g., expansion of agriculture and urban areas) since 2009 and a 96% increase since 1985 (Chesapeake Bay Program 2021) which has been shown to enhance DOC degradation in other estuaries (Wu et al. 2019; Asmala et al. 2013; Petrone et al. 2009).

The upper range of ΔDOC (− 34 to − 41%) was measured during October (Fig. 3a; Table S6). Similar losses of DOC during incubation studies have been reported in the Clyde River Estuary, Australia (ΔDOC = − 3 to − 31%; Hitchcock and Mitrovic 2015), Chilika Lagoon, India (ΔDOC = − 25 to − 62%; Kanuri et al. 2018), the Pearl River Estuary, China (ΔDOC = − 16 to − 43%; He et al. 2010) (Table 3), and in streams, tidal creeks, and marshes that drain into estuaries (Wu et al. 2021; Fork et al. 2020; Cammer 2015). In all of these cases, high ΔDOC (%) was partially attributed to inputs of nutrients and labile organic matter from freshwater inflows that supported the microbial community. During October in our study, the combination of average flow conditions and DOC derived from aquatic, microalgal sources may have also been optimal for high ΔDOC (%).

In this study, changes in [DOC] were assumed to be driven by microbial processes since incubations were conducted in the dark, and uninoculated treatments (0.2 µm filtrate only) did not show significant changes in [DOC] over time (Table S7). Fortin et al. (2021) reported seasonal shifts in microbial community composition in work conducted at the same sampling periods and locations as this study. Rates of

Table 3 Selected studies that measured DOC degradation in estuaries and coastal environments using similar experimental methods and analyses

Location	Incubation length (days)	Incubation temperatures (°C)	ΔDOC (%)	Reference
York River Estuary, VA, USA	28	4, 12, 25, 29	0–41	This study
York River Estuary, VA, USA	28	22	3–12	McCallister et al. (2006)
Headwaters of the York River Estuary, VA, USA	35–36	22	0–24	Lu et al. (2013)
Changjiang Estuary, China	52–58	Room temperature	13–20	Ji et al. (2021)
Lavaca, San Antonio, Mission, Aransas, and Nueces Rivers, Texas, USA	24	14, 31	0–11	Wu et al. (2019)
Clyde River Estuary, Australia	28	20	3–31	Hitchcock and Mitrovic (2015)
Chilika Lagoon, India	90	25	25–62	Kanuri et al. (2018)
Karjaanjoki, Kyrönjoki and Kiiminkijoki estuaries, Finland	10–12	4, 10, 18	3–11	Asmala et al. (2013)
Pearl River Estuary, China	30	20	16–43	He et al. (2010)
Swan-Canning Estuary, Perth, Western Australia	14	25	1–17	Petrone et al. (2009)
San Francisco Estuary, CA, USA	21	Room temperature	11–15	Sobczak et al. (2002)
Cape Fear River Estuary, NC, USA	21	In situ (not specified)	1–14	Avery et al. (2003)
Satila River Estuary, Georgia, USA	51	20	3–9	Moran et al. (2000)
Altamaha River Estuary, GA, USA	60	24	9–12	Martineac et al. (2021)
Savannah, Ogeechee, Altamaha, Satila, and St. Marys Rivers, southeast USA	35–58	20	2–18	Moran et al. (1999)

N cycling processes measured by Fortin et al. (2021) were higher in fall and summer, consistent with our findings that microbial degradation of DOC was higher in October and July. Particularly, ammonia and nitrite-oxidizing archaea and bacteria comprised nearly 20% of the YRE microbial community during October 2018 (Fortin, unpub. data). Prior work has shown that similar coastal and marine microbial communities can release a diverse suite of bioavailable CDOM components (Arai et al. 2018; Lønberg et al. 2009). As a result, the microbes in our study may have produced easily degraded DOC components as evidenced by the high protein-like CDOM fluorescence measured in October (Fig. 2j; Table S3).

Our multiple linear regression model revealed that DOC degradation was best explained by $\delta^{13}C_{DOC}$ values, water temperature, flushing time, and freshwater age (Table 2). Samples with higher contributions of autochthonous DOC had higher rates of degradation and samples with higher contributions of allochthonous DOC had lower rates of degradation. Further, the tidal freshwater sampling location (Fig. 1), which represents possible inputs of more terrestrial DOM from the watershed into the YRE, had lower ΔDOC (%) than the mainstem YRE during October when degradation was otherwise the highest (Fig. S3). In contrast, ΔDOC (%) at the tidal freshwater location in February was similar to the mainstem YRE when degradation was the lowest and contributions of terrestrial DOC to the estuary were highest (Fig. S3). These relative differences in reactivity between autochthonous and allochthonous DOC are consistent with our hypothesis, previous work in the YRE (McCallister et al. 2006), and dynamically similar systems such as estuaries in coastal Georgia (Martineac et al. 2021; Moran et al. 1999), Texas (Wu et al. 2019), and California (Sobczak et al. 2002).

Chlorophyll-*a*, a common proxy for phytoplankton production in the YRE (Lake and Brush 2015) and other estuaries (Ji et al. 2021; He et al. 2020), did not correlate with ΔDOC (%) and did not emerge as a significant predictor during the multiple linear regression analysis even though we attributed more DOC degradation to autochthonous sources of DOC. This mismatch may be due to the decoupling of spatial and temporal dynamics in biogeochemical parameters during altered freshwater discharge conditions (e.g., patterns in DOC, DON, and DIC concentrations versus patterns in NO_x, NH_4^+, and chlorophyll-*a* concentrations). Additionally, phytoplankton-derived DOC may not be accurately reflected by chlorophyll-*a* concentrations because chlorophyll-*a* quickly degrades and is transformed during grazing processes (Sheer 2012; Szymczak-Żyla et al. 2008). It is also possible that DOC may have been derived from non-photosynthetic and non-chlorophyll-containing organisms (Sánchez-Pérez et al. 2020; Hopkinson et al. 2002). Overall, $\delta^{13}C_{DOC}$ values seemed to be a better predictor of degradation in this study because they provided an integrated measure of DOC sources.

Temperature was relatively equal to $\delta^{13}C_{DOC}$ in its ability to predict DOC degradation (Table 2). We generally measured higher rates of degradation in October and July when surface water and incubation temperatures were warm (25–29 °C) compared to February and April when temperatures were cooler (4–12 °C) (Fig. 5b). Previous studies have shown that higher rates of respiration and the metabolic breakdown of organic matter are typically strongly correlated with higher temperatures (Hopkinson and Smith 2005 and references therein). However, many previous studies have kept temperature constant across seasons thereby measuring "potential" reactivity (e.g., McCallister et al. 2006; Lu et al. 2013). In this study, we incubated samples at ambient temperatures. As a result, the effect of temperature on DOC reactivity highlights the importance of temporal differences in ΔDOC (%) naturally captured in our seasonal study.

Estuarine hydrology exerts a strong control on the sources and residence time of DOC delivered to an estuary and the associated biological processes that follow (Bianchi 2007). In our study, time periods with high freshwater ages were dominated by autochthonous DOC sources while lower freshwater ages were dominated by allochthonous sources (Fig. 6). While freshwater age and ΔDOC (%) did not correlate directly with one another, these results support our original hypothesis that freshwater discharge affects DOC source which thereby influences rates of DOC degradation. This corroborates other studies that have found freshwater discharge, residence time (Wu et al. 2019; Kanuri et al. 2018; Hitchcock and Mitrovic 2015), and DOC source and chemical composition (Ji et al. 2021; McCallister et al. 2006) collectively contribute to DOC reactivity.

During the February incubation experiments, we observed a slight increase in [DOC] in the middle ($\Delta DOC = 2.90 \pm 0.48\%$) and lower ($\Delta DOC = 13.9 \pm 23.0\%$) estuary (Fig. 3a; Table S6) which is not often reported for dark incubation experiments. However, we should note that observed increases in [DOC] were not significantly different from zero. DIN ($NH_4^+ + NO_x$) concentrations were higher in February compared to April and July, which may have supported the growth of the previously described ammonia and nitrite oxidizing microbes and the subsequent release of DOC into estuarine surface waters (Bayer et al. 2023, 2019; Pachiadaki et al. 2017). It is also possible that the combination of low incubation temperature and large amounts of terrestrial DOC along the YRE in February inhibited the microbial degradation of DOC and supported the chemolithoautotrophic oxidation of inorganic compounds to produce DOC (Dang and Chen 2017).

Overall, this study captured average to wet conditions, so it is uncertain how anomalously dry conditions may have impacted the physical and biogeochemical conditions of the YRE and subsequent DOM degradation. Other studies have shown that prolonged dry conditions limit nutrient

inputs and organic matter production in estuaries (Douglas et al. 2023), resulting in a higher prevalence of DOM inputs from marine sources or passive exchange processes (e.g., lateral inputs of tidal marsh-derived DOM) (Medeiros et al. 2015). As a result, the effect of prolonged dry conditions on DOM reactivity depends on physical and biogeochemical responses of estuaries and their surrounding watershed features to minimal or no freshwater discharge (Medeiros et al. 2017; Vazquez et al. 2011).

DON and CDOM Degradation

DON was lost at a rate up to six times lower than DOC across all sampling periods (excluding October when DON was not measured). We also observed that DON was produced rather than degraded during the April incubations (Fig. 3b; Table S6). Chemosynthetic processes may explain the production of DON during April 2019 (Ji et al. 2021; Wu et al. 2019). In a companion study conducted in April 2019, Stanley (2021) reported high rates of NH_4^+ uptake coinciding with the *H. triquetra* bloom, suggesting that phytoplankton and bacteria were active during this time and may have leached or produced DON (Liao et al. 2019; Eom et al. 2017). This could also explain why [NH_4^+] emerged as an important predictor variable in the multiple linear regression analysis (Table 2). Alternatively, prior work has shown that other microbial processes such as N_2 fixation can be an important source of DON to coastal and marine waters (Sipler and Bronk 2015 and references therein; Voss et al. 2013).

Previous studies have shown that DON can be reactive during periods of high freshwater discharge and when concentrations of inorganic nutrients (NO_x and NH_4^+) are low (Pisani et al. 2017; Garcia et al. 2015). In studies that have compared reactivities of DOC to DON, DON was sometimes more reactive and sensitive to changing environmental conditions (Wu et al. 2019; Asmala et al. 2013; Petrone et al. 2009; Wiegner and Seitzinger 2001). Other studies have measured relatively equal reactivities (Kanuri et al. 2018) or a more reactive DOC pool (Knudsen-Leerback et al. 2017). In each of these cases, differences in reactivity depended on estuarine morphology and DON source (Seitzinger et al. 2002; Wiegner and Seitzinger 2001).

DON degradation was primarily explained by slope ratio (S_R) and flushing time (Table 2). Overall, higher S_R (lower molecular weight DOM derived from autochthonous sources) and lower flushing times were associated with higher rates of DON degradation (Fig. 7). As was the case with DOC, CDOM composition provided insights about DON source, composition, and subsequent reactivity, reinforcing its utility in investigating estuarine DOM dynamics (Osburn et al. 2016b; Heinz et al. 2015). Though not strongly correlated with ΔDON (%), the inclusion of protein-like and humic-like CDOM fluorescence, chlorophyll-*a*, [DOC], and pH in the multiple linear regression analysis resulted in a more robust model (large variance explained, no collinearity, low AICc) for explaining DON degradation. It is possible that the optical properties of DOM considered in this study characterize DON better than DOC, especially as it pertains to source and reactivity (Li et al. 2021; Wymore et al. 2018; Osburn et al. 2016b). Concentrations of DOC and chlorophyll-*a* and pH were less important in the model. Excluding them only reduced the adjusted r^2 value by ~ 0.06 but increased the AICc value by ~ 20. Therefore, we chose to keep them in the final model for broader applicability to other systems and to balance over and underfitting the data following the theoretical foundations for AIC (Cavanaugh and Neath 2018; Akaike 1998).

The degradation of protein-like CDOM derived from microbial sources was similar in magnitude to DOC degradation in October and July (Figs. 3a and 4a). On the other hand, protein-like CDOM degradation was highly variable during February and April particularly in the middle estuary where protein-like CDOM was produced (Fig. 4a; Table S6). This variability may be attributed to the middle estuary sampling location since it coincides with the YRE's secondary turbidity maximum (STM) where substantial sediment resuspension and frequent winter and spring phytoplankton blooms occur (Reay 2009; Sin et al. 1999). Except for these instances when protein-like CDOM was produced, overall higher losses of protein-like CDOM relative to humic-like CDOM were consistent with our finding that DOM derived from aquatic, autochthonous sources was more reactive than DOM derived from terrestrial, allochthonous sources. In fact, protein-like CDOM had a positive linear relationship with ΔDOC (%) (adj. $r^2 = 37$; $p < 0.01$) but did not strengthen the multiple linear regression model for ΔDOC (%) (Table S1).

Instances of CDOM production (> 300% of initial fluorescence intensities) that were consistent across replicates and that primarily occurred between 0 and 1 incubation days were observed during July in the humic-like CDOM pool (Fig. 4b; Table S6; Fig. S1d). Previous work has shown that humification processes during incubation experiments can cause sorption of proteinaceous or amino acid-like CDOM to humic-like CDOM components, resulting in increased fluorescence over time (Santos et al. 2016; Guillemette and del Giorgio 2012; Boyd and Osburn 2004). On the other hand, degradation was high in the upper estuary during July for humic-like CDOM (ΔCDOM = − 64 to − 67%) and represented the largest loss of all measured DOM pools during the study period (Fig. 4; Table S6). Large decreases in CDOM have previously been observed during incubations of estuarine surface waters particularly near freshwater endmembers (Moran et al. 2000). In our study, July experienced the lowest flushing time and highest freshwater age among

all sampling dates, potentially causing enhanced CDOM degradation in the upper estuary and enhanced CDOM accumulation in the lower estuary. Otherwise, the occurrence and high variability in both CDOM production and degradation could be attributed to fine-scale alterations of CDOM (Boyd and Osburn 2004) or the synchronous production and degradation of distinct CDOM components (Kadjeski et al. 2020).

Taken together, CDOM was a good proxy for DOM source and composition, but rates of CDOM degradation were often inconsistent with DOC and DON degradation. Previous studies have also shown that CDOM degradation is not always a good predictor of DOM degradation (e.g., Cammer 2015; Minor et al. 2014; Boyd and Osburn 2004). This may be due to high uncertainty and variation across incubation replicates, sampling locations, and seasons (Fig. 4; Table S6); interactions between different moieties and the "dark" and fluorescent pools of DOM (Stubbins et al. 2014); and potentially small contributions of CDOM and fDOM to the total DOM pool (Nelson and Siegel 2013; Coble 2007). Therefore, optical properties of DOM provide limited but nonetheless useful insight into understanding bulk DOM reactivity and estuarine biogeochemistry. As a result, analyzing individual fractions of the DOM pool (e.g., lipids, amino acids) or using higher resolution techniques (e.g., mass spectrometry) to describe DOM in more detail may better elucidate how DOM source and composition affect degradation.

Summary and Conclusion

This study aimed to determine physical and biogeochemical controls on surface water DOM reactivity along the YRE, a sub-estuary of the Chesapeake Bay in southeast Virginia and representative of temperate, microtidal systems common along the east coast of the USA. While the October 2018 and July 2019 sampling periods represented typical environmental conditions, the YRE and broader Chesapeake Bay region was characterized by prolonged wet conditions throughout 2018 and 2019, particularly during the February and April 2019 sampling periods. As a result, this seasonal study showed that changing hydrologic conditions of the YRE affected surface water biogeochemistry, DOM source and composition, and subsequent DOM degradation. Our incubation experiments revealed higher ΔDOC (%) when estuarine phytoplankton sources dominated (e.g., more positive $\delta^{13}C_{DOC}$), temperatures were warmer, and flushing times were longer. In comparison, we measured lower ΔDOC (%) when contributions of DOC from terrestrial sources were more abundant (e.g., more negative $\delta^{13}C_{DOC}$), temperatures were cooler, and flushing times were shorter.

We found that DOC, DON, and CDOM had different reactivities across space and time most likely because each pool is comprised of different compounds with varying responses to changing environmental conditions. DON was lost at a rate up to six times lower than DOC, and DON was sometimes produced rather than degraded during the incubations. CDOM degradation was highly variable, and optical properties of DOM described DOC and DON differently. This inconsistency highlights the limitations of using CDOM as a proxy for DOC and DON reactivity. Despite differences in DOC, DON, and CDOM reactivity across the sample dates, microbial degradation of DOM was best predicted by similar variables at least for DOC and DON. These included physical controls (i.e., flushing time, freshwater age) and biogeochemical controls (i.e., DOM source and chemical composition).

The mid-Atlantic region of the USA is projected to experience higher annual rates of precipitation, greater frequency of extreme storm events, and warming temperatures over the next several decades (Bradley et al. 2016; Najjar et al. 2010). Based on our results, higher freshwater discharge associated with more precipitation and storm events will likely decrease estuarine flushing time and freshwater age, resulting in higher delivery of allochthonous DOM into coastal waters, and lower rates of DOM degradation. At the same time, warming temperatures are expected to increase rates of DOM degradation, highlighting the unknown interplay between changing environmental conditions and their effect on the coastal carbon cycle.

Supplementary Information The online version contains supplementary material available at https://doi.org/10.1007/s12237-024-01474-0.

Acknowledgements We would like to thank many individuals at VIMS who assisted with field work and laboratory experiments, including fellow "Lyrettes" Samantha Fortin, Stephanie Peart, Hunter Walker, Stephanie Wilson, and Michelle Woods. We thank Chris Osburn and the North Carolina State Aquatic Biogeochemistry laboratory for the stable isotope analyses. We would like to acknowledge Kimberly Reece and Bongkeun Song as co-principal investigators involved with the NSF BIO-OCE project from which this project stemmed. We thank the five anonymous reviewers for providing thoughtful feedback on this manuscript. We dedicate this manuscript to the memory of I. Anderson, who was instrumental in the conceptualization, development, execution, and completion of this project.

Funding This project was funded by grants awarded to I. Anderson (NSF BIO-OCE #1737258) and D. Detweiler (Virginia Water Resources Research Center).

Data Availability The data that support the findings of this study are available within the article, its supplementary materials, and from the corresponding author upon reasonable request.

Declarations

Competing Interests The authors declare no competing interests.

References

Akaike, H. 1998. Information theory and an extension of the maximum likelihood principle. In: Parzen, E., Tanabe, K., Kitagawa, G. (eds) Selected papers of Hirotugu Akaike. Springer Series in Statistics. Springer, New York, NY. https://doi.org/10.1007/978-1-4612-1694-0_15.

Anderson, I., K. McGlathery, and A. Tyler. 2003. Microbial mediation of reactive nitrogen transformations in a temperate lagoon. *Marine Ecology Progress Series* 246: 73–84. https://doi.org/10.3354/meps246073.

Andersson, A., S. Brugel, J. Paczkowska, O.F. Rowe, D. Figueroa, S. Kratzer, and C. Legrand. 2018. Influence of allochthonous dissolved organic matter on pelagic basal production in a northerly estuary. *Estuarine, Coastal and Shelf Science* 204: 225–235. https://doi.org/10.1016/j.ecss.2018.02.032.

Arai, K., S. Wada, K. Shimotori, Y. Omori, and T. Hama. 2018. Production and degradation of fluorescent dissolved organic matter derived from bacteria. *Journal of Oceanography* 74: 39–52. https://doi.org/10.1007/s10872-017-0436-y.

Asmala, E., R. Autio, H. Kaartokallio, L. Pitkänen, C.A. Stedmon, and D.N. Thomas. 2013. Bioavailability of riverine dissolved organic matter in three Baltic Sea estuaries and the effect of catchment land use. *Biogeosciences* 10: 6969–6986. https://doi.org/10.5194/bg-10-6969-2013.

Avery, G. B., J. D. Willey, R. J. Kieber, G. C. Shank, and R. F. Whitehead. 2003. Flux and bioavailability of Cape Fear River and rainwater dissolved organic carbon to Long Bay, southeastern United States. *Global Biogeochemical Cycles* 17. https://doi.org/10.1029/2002GB001964

Bauer, J.E., and T. S. Bianchi. 2011. Dissolved organic carbon cycling and transformation. In *Treatise on Estuarine and Coastal Science*, 7–67. Elsevier. https://doi.org/10.1016/B978-0-12-374711-2.00502-7.

Bayer, B., R.L. Hansman, M.J. Bittner, B.E. Noriega-Ortega, J. Niggemann, T. Dittmar, and G.J. Herndl. 2019. Ammonia-oxidizing archaea release a suite of organic compounds potentially fueling prokaryotic heterotrophy in the ocean. *Environmental Microbiology* 21: 4062–4075. https://doi.org/10.1111/1462-2920.14755.

Bayer, B., K. McBeain, C.A. Carlson, and A.E. Santoro. 2023. Carbon content, carbon fixation yield and dissolved organic carbon release from diverse marine nitrifiers. *Limnology and Oceanography* 68: 84–96. https://doi.org/10.1002/lno.12252.

Bianchi, T.S. 2011. The role of terrestrially derived organic carbon in the coastal ocean: A changing paradigm and the priming effect. *Proceedings of the National Academy of Sciences* 108: 19473–19481. https://doi.org/10.1073/pnas.1017982108.

Bianchi, T. S. 2007. *Biogeochemistry of estuaries*. Oxford; New York: Oxford University Press.

Borges, A. V., and G. Abril. 2011. Carbon dioxide and methane dynamics in estuaries. In *Treatise on Estuarine and Coastal Science*, 119–161. Elsevier. https://doi.org/10.1016/B978-0-12-374711-2.00504-0.

Boyd, T.J., and C.L. Osburn. 2004. Changes in CDOM fluorescence from allochthonous and autochthonous sources during tidal mixing and bacterial degradation in two coastal estuaries. *Marine Chemistry* 89: 189–210. https://doi.org/10.1016/j.marchem.2004.02.012.

Bradley, R., A. Karmalkar, and K. Woods. 2016. How will global warming of 2°C affect Virginia? Observed and projected changes in climate and their impacts. Climate System Research Center. University of Massachusetts Amherst. https://www.geo.umass.edu/climate/stateClimateReports/VA_ClimateReport_CSRC.pdf. Accessed 17 April 2023

Bronk, D., and P. Gilbert. 1993. Contrasting patterns of dissolved organic nitrogen release by two size fractions of estuarine plankton during a period of rapid NH_4^+ consumption and $N0_2^-$ production. *Marine Ecology Progress Series* 96: 291–299. https://doi.org/10.3354/meps096291.

Bukaveckas, P.A. 2022. Carbon dynamics at the river–estuarine transition: A comparison among tributaries of Chesapeake Bay. *Biogeosciences* 19: 4209–4226. https://doi.org/10.5194/bg-19-4209-2022.

Cai, W.-J. 2011. Estuarine and coastal ocean carbon paradox: CO_2 sinks or sites of terrestrial carbon incineration? *Annual Review of Marine Science* 3: 123–145. https://doi.org/10.1146/annurev-marine-120709-142723.

Cammer, S. S. 2015. Storm event impact on organic matter flux, composition and reactivity in Taskinas Creek, VA. *Dissertations, Theses, and Masters Projects*. William & Mary. Paper 1477068589. https://doi.org/10.21220/V5HS4G.

Canuel, E.A., and A.K. Hardison. 2016. Sources, ages, and alteration of organic matter in estuaries. *Annual Review of Marine Science* 8: 409–434. https://doi.org/10.1146/annurev-marine-122414-034058.

Carlson, C. A., and D. A. Hansell. 2015. DOM sources, sinks, reactivity, and budgets. In Biogeochemistry of Marine Dissolved Organic Matter, 65–126. Elsevier. https://doi.org/10.1016/B978-0-12-405940-5.00003-0.

Cavanaugh, J. E., and A. A. Neath. 2018. The Akaike information criterion: Background, derivation, properties, application, interpretation, and refinements. *WIREs Computational Statistics*: e1460. https://doi.org/10.1002/wics.1460.

Chesapeake Bay Foundation. 2020. State of the Bay 2020. https://www.cbf.org/document-library/cbf-reports/2020-state-of-the-bay-report.pdf. Accessed 27 June 2023.

Chesapeake Bay Program. 2021. York tributary summary: A summary of trends in tidal water quality and associated factors 1985–2018. https://cast-content.chesapeakebay.net/documents/TribSummaries_YorkTributaryTrendsSummary2021-06-07.pdf. Accessed 17 April 2023.

Chow, A.T.-S., Y. Ulus, G. Huang, M.A. Kline, and W.-Y. Cheah. 2022. Challenges in quantifying and characterizing dissolved organic carbon: Sampling, isolation, storage, and analysis. *Journal of Environmental Quality* 51 (5): 837–871. https://doi.org/10.1002/jeq2.20392.

Cloern, J.E., E.A. Canuel, and D. Harris. 2002. Stable carbon and nitrogen isotope composition of aquatic and terrestrial plants of the San Francisco Bay estuarine system. *Limnology and Oceanography* 47: 713–729. https://doi.org/10.4319/lo.2002.47.3.0713.

Cloern, J.E., S.Q. Foster, and A.E. Kleckner. 2014. Phytoplankton primary production in the world's estuarine-coastal ecosystems.

Biogeosciences 11: 2477–2501. https://doi.org/10.5194/bg-11-2477-2014.

Coble, P.G. 1996. Characterization of marine and terrestrial DOM in seawater using excitation-emission matrix spectroscopy. *Marine Chemistry* 51: 325–346. https://doi.org/10.1016/0304-4203(95)00062-3.

Coble, P.G. 2007. Marine optical biogeochemistry: The chemistry of ocean color. *Chemical Reviews* 107: 402–418. https://doi.org/10.1021/cr050350+.

Countway, R.E., E.A. Canuel, and R.M. Dickhut. 2007. Sources of particulate organic matter in surface waters of the York River, VA estuary. *Organic Geochemistry* 38: 365–379. https://doi.org/10.1016/j.orggeochem.2006.06.004.

Crosswell, J.R., I.C. Anderson, J.W. Stanhope, B. Van Dam, M.J. Brush, S. Ensign, M.F. Piehler, B. McKee, M. Bost, and H.W. Paerl. 2017. Carbon budget of a shallow, lagoonal estuary: Transformations and source-sink dynamics along the river-estuary-ocean continuum: Carbon budget of a shallow estuary. *Limnology and Oceanography* 62: S29–S45. https://doi.org/10.1002/lno.10631.

Dang, H., and C.-T.A. Chen. 2017. Ecological energetic perspectives on responses of nitrogen-transforming chemolithoautotrophic microbiota to changes in the marine environment. *Frontiers in Microbiology* 8: 1246. https://doi.org/10.3389/fmicb.2017.01246.

Del Vecchio, R., and N.V. Blough. 2004. Spatial and seasonal distribution of chromophoric dissolved organic matter and dissolved organic carbon in the Middle Atlantic Bight. *Marine Chemistry* 89: 169–187. https://doi.org/10.1016/j.marchem.2004.02.027.

Douglas, S., J. Xue, A. Hardison, and Z. Liu. 2023. Phytoplankton community response to a drought-to-wet climate transition in a subtropical estuary. *Limnology and Oceanography* 68: https://doi.org/10.1002/lno.12348.

Eom, H., D. Borgatti, H.W. Paerl, and C. Park. 2017. Formation of low-molecular-weight dissolved organic nitrogen in predenitrification biological nutrient removal systems and its impact on eutrophication in coastal waters. *Environmental Science & Technology* 51: 3776–3783. https://doi.org/10.1021/acs.est.6b06576.

Fasching, C., B. Behounek, G.A. Singer, and T.J. Battin. 2014. Microbial degradation of terrigenous dissolved organic matter and potential consequences for carbon cycling in brown-water streams. *Scientific Reports* 4: 4981. https://doi.org/10.1038/srep04981.

Fichot, C.G., and R. Benner. 2012. The spectral slope coefficient of chromophoric dissolved organic matter (S 275–295) as a tracer of terrigenous dissolved organic carbon in river-influenced ocean margins. *Limnology and Oceanography* 57: 1453–1466. https://doi.org/10.4319/lo.2012.57.5.1453.

Fork, M.L., C.L. Osburn, and J.B. Heffernan. 2020. Bioavailability and compositional changes of dissolved organic matter in urban headwaters. *Aquatic Sciences* 82: 66. https://doi.org/10.1007/s00027-020-00739-7.

Fortin, S.G., B. Song, and I. C. Anderson. 2021. Microbially mediated nitrogen removal and retention in the York River Estuary. *FEMS Microbiology Ecology* 97: fiab118. https://doi.org/10.1093/femsec/fiab118.

Frankel, L.T., M.A.M. Friedrichs, P. St-Laurent, A.J. Bever, R.N. Lipcius, G. Bhatt, and G.W. Shenk. 2022. Nitrogen reductions have decreased hypoxia in the Chesapeake Bay: Evidence from empirical and numerical modeling. *Science of the Total Environment* 814: 152722. https://doi.org/10.1016/j.scitotenv.2021.152722.

Friedrichs, C.T. 2009. York River physical oceanography and sediment transport. *Journal of Coastal Research* 10057: 17–22. https://doi.org/10.2112/1551-5036-57.sp1.17.

Fry, B., and E. B. Sherr. 1984. $\delta^{13}C$ measurements as indicators of carbon flow in marine and freshwater ecosystems. In *Stable isotopes in ecological research*, ed. P. W. Rundel, J. R. Ehleringer, and K. A. Nagy, 196–229. New York, NY: Springer New York.

Garcia, J.C., R.D.J. Ketover, A.N. Loh, M.L. Parsons, and H. Urakawa. 2015. Influence of freshwater discharge on the microbial degradation processes of dissolved organic nitrogen in a subtropical estuary. *Antonie Van Leeuwenhoek* 107: 613–632. https://doi.org/10.1007/s10482-014-0357-3.

Graeber, D., Y. Tenzin, M. Stutter, G. Weigelhofer, T. Shatwell, W. Von Tümpling, J. Tittel, A. Wachholz, and D. Borchardt. 2021. Bioavailable DOC: Reactive nutrient ratios control heterotrophic nutrient assimilation—An experimental proof of the macronutrient-access hypothesis. *Biogeochemistry* 155: 1–20. https://doi.org/10.1007/s10533-021-00809-4.

Guillemette, F., and P.A. del Giorgio. 2012. Simultaneous consumption and production of fluorescent dissolved organic matter by lake bacterioplankton: Bacterial production and consumption of FDOM. *Environmental Microbiology* 14: 1432–1443. https://doi.org/10.1111/j.1462-2920.2012.02728.x.

He, B., M. Dai, W. Zhai, L. Wang, K. Wang, J. Chen, J. Lin, A. Han, and Y. Xu. 2010. Distribution, degradation and dynamics of dissolved organic carbon and its major compound classes in the Pearl River estuary, China. *Marine Chemistry* 119: 52–64. https://doi.org/10.1016/j.marchem.2009.12.006.

He, C., Q. Pan, P. Li, W. Xie, D. He, C. Zhang, and Q. Shi. 2020. Molecular composition and spatial distribution of dissolved organic matter (DOM) in the Pearl River Estuary. *China. Environmental Chemistry* 17: 240. https://doi.org/10.1071/EN19051.

Hedges, J.I., and R.G. Keil. 1999. Organic geochemical perspectives on estuarine processes: Sorption reactions and consequences. *Marine Chemistry* 65: 55–65. https://doi.org/10.1016/S0304-4203(99)00010-9.

Heinz, M., D. Graeber, D. Zak, E. Zwirnmann, J. Gelbrecht, and M.T. Pusch. 2015. Comparison of organic matter composition in agricultural versus forest affected headwaters with special emphasis on organic nitrogen. *Environmental Science & Technology* 49: 2081–2090. https://doi.org/10.1021/es505146h.

Helms, J.R., A. Stubbins, J.D. Ritchie, E.C. Minor, D.J. Kieber, and K. Mopper. 2008. Absorption spectral slopes and slope ratios as indicators of molecular weight, source, and photobleaching of chromophoric dissolved organic matter. *Limnology and Oceanography* 53: 955–969. https://doi.org/10.4319/lo.2008.53.3.0955.

Hitchcock, J.N., and S.M. Mitrovic. 2015. After the flood: Changing dissolved organic carbon bioavailability and bacterial growth following inflows to estuaries. *Biogeochemistry* 124: 219–233. https://doi.org/10.1007/s10533-015-0094-3.

Holmer, M. 1996. Composition and fate of dissolved organic carbon derived from phytoplankton detritus in coastal marine sediments. *Marine Ecology Progress Series* 141: 217–228. https://doi.org/10.3354/meps141217.

Hopkinson, C.S., J.J. Vallino, and A. Nolin. 2002. Decomposition of dissolved organic matter from the continental margin. *Deep Sea Research II* 49 (20): 4461–4478. https://doi.org/10.1016/S0967-0645(02)00125-X.

Hopkinson, C. S., and E. M. Smith. 2005. Estuarine respiration: An overview of benthic, pelagic, and whole system respiration. In *Respiration in Aquatic Ecosystems*, ed. P. del Giorgio and P. Williams, 122–146. Oxford University Press. https://doi.org/10.1093/acprof:oso/9780198527084.003.0008.

Hopkinson, C. S., I. Buffam, J. Hobbie, J. Vallino, M. Perdue, B. Eversmeyer, F. Prahl, et al. 1998. Terrestrial inputs of organic matter to coastal ecosystems: An intercomparison of chemical characteristics and bioavailability. *Biogeochemistry* 43: 211–234. http://www.jstor.org/stable/1469425.

Hounshell, A.G., J.C. Rudolph, B.R. Van Dam, N.S. Hall, C.L. Osburn, and H.W. Paerl. 2019. Extreme weather events modulate processing and export of dissolved organic carbon in the Neuse River

Estuary, NC. *Estuarine, Coastal and Shelf Science* 219: 189–200. https://doi.org/10.1016/j.ecss.2019.01.020.

Hudson, N., A. Baker, and D. Reynolds. 2007. Fluorescence analysis of dissolved organic matter in natural, waste and polluted waters—A review. *River Research and Applications* 23: 631–649. https://doi.org/10.1002/rra.1005.

Jakobsen, H.H., and S. Markager. 2016. Carbon-to-chlorophyll ratio for phytoplankton in temperate coastal waters: Seasonal patterns and relationship to nutrients. *Limnology and Oceanography* 61 (5): 1853–1868. https://doi.org/10.1002/lno.10338.

Ji, C., Y. Chen, and G. Yang. 2021. Seasonal variation, degradation, and bioavailability of dissolved organic matter in the Changjiang Estuary and its adjacent East China Sea. *Journal of Geophysical Research: Oceans* 126. https://doi.org/10.1029/2020JC016648.

Kadjeski, M., C. Fasching, and M.A. Xenopoulos. 2020. Synchronous biodegradability and production of dissolved organic matter in two streams of varying land use. *Frontiers in Microbiology* 11: 568629. https://doi.org/10.3389/fmicb.2020.568629.

Kanuri, V. V., P. R. Muduli, R. R.S., C. K. B., L. R. A., S. Patra, G. V. M. Gupta, G. Nageswara Rao, R. A.V., and S. B.R. 2018. Bioavailable dissolved organic matter and its spatio-temporal variation in a river dominated tropical brackish water Lagoon, India. *Marine Pollution Bulletin* 131: 460–467. https://doi.org/10.1016/j.marpolbul.2018.04.059

Kim, J., M.J. Brush, B. Song, and I.C. Anderson. 2021. Reconstructing primary production in a changing estuary: A mass balance modeling approach. *Limnology and Oceanography* 66: 2535–2546. https://doi.org/10.1002/lno.11771.

Knobloch, A. L. J., P. J. Neale, M. Tzortziou, and E. A. Canuel. 2022. Seasonal and tidal controls of the quantity and quality of dissolved organic matter at the marsh creek-estuarine interface. *Estuarine, Coastal and Shelf Science* 278. https://doi.org/10.1016/j.ecss.2022.108124

Knudsen-Leerbeck, H., M. Mantikci, M. Bentzon-Tilia, S.J. Traving, L. Riemann, J.L.S. Hansen, and S. Markager. 2017. Seasonal dynamics and bioavailability of dissolved organic matter in two contrasting temperate estuaries. *Biogeochemistry* 134: 217–236. https://doi.org/10.1007/s10533-017-0357-2.

Koroleff, F. 1983. Determination of nutrients. In *Methods of Seawater Analysis*, 2nd ed., 125–187. Weinheim: VerlagChemie.

Lake, S.J., and M.J. Brush. 2015. Contribution of nutrient and organic matter sources to the development of periodic hypoxia in a tributary estuary. *Estuaries and Coasts* 38: 2149–2171. https://doi.org/10.1007/s12237-015-9954-2.

Lake, S., M. Brush, I. Anderson, and H. Kator. 2013. Internal versus external drivers of periodic hypoxia in a coastal plain tributary estuary: The York River, Virginia. *Marine Ecology Progress Series* 492: 21–39. https://doi.org/10.3354/meps10468.

Lawaetz, A.J., and C.A. Stedmon. 2009. Fluorescence intensity calibration using the Raman scatter peak of water. *Applied Spectroscopy* 63: 936–940. https://doi.org/10.1366/000370209788964548.

Letourneau, M.L., S.C. Schaefer, H. Chen, A.M. McKenna, M. Alber, and P.M. Medeiros. 2021. Spatio-temporal changes in dissolved organic matter composition along the salinity gradient of a marsh-influenced estuarine complex. *Limnology and Oceanography* 66: 3040–3054. https://doi.org/10.1002/lno.11857.

Li, D., B. Pan, X. Han, J. Li, Q. Zhu, and M. Li. 2021. Assessing the potential to use CDOM as an indicator of water quality for the sediment-laden Yellow river. *China. Environmental Pollution* 289 (15): 117970. https://doi.org/10.1016/j.envpol.2021.117970.

Liao, K., H. Hu, S. Ma, and H. Ren. 2019. Effect of microbial activity and microbial community structure on the formation of dissolved organic nitrogen (DON) and bioavailable DON driven by low temperatures. *Water Research* 159: 397–405. https://doi.org/10.1016/j.watres.2019.04.049.

Liao, N. 2001. Determination of ammonia in brackish or seawater by flow injection analysis. QuikChem Method 31–107–06–1-B. Milwaukee: Lachat Instruments.

Lindholm, T., and C. Nummelin. 1999. Red tide of the dinoflagellate *Heterocapsa triquetra* (Dinophyta) in a ferry-mixed coastal inlet. *Hydrobiologia* 393: 245–251. https://doi.org/10.1023/A:1003563022422.

Litaker, R., P. Tester, C. Duke, B. Kenney, J. Pinckney, and J. Ramus. 2002. Seasonal niche strategy of the bloom-forming dinoflagellate Heterocapsa triquetra. *Marine Ecology Progress Series* 232: 45–62. https://doi.org/10.3354/meps232045.

Logozzo, L., M. Tzortziou, P. Neale, and J. B. Clark. 2021. Photochemical and microbial degradation of chromophoric dissolved organic matter exported from tidal marshes. *Journal of Geophysical Research: Biogeosciences* 126. https://doi.org/10.1029/2020JG005744.

Lønberg, C., X.A. Álvarez-Salgado, K. Davidson, and A.E.J. Miller. 2009. Production of bioavailable and refractory dissolved organic matter by coastal heterotrophic microbial populations. *Estuarine, Coastal and Shelf Science* 82 (4): 682–688. https://doi.org/10.1016/j.ecss.2009.02.026.

Lønberg, C., X.A. Álvarez-Salgado, K. Davidson, S. Martínez-García, and E. Teira. 2010. Assessing the microbial bioavailability and degradation rate constants of dissolved organic matter by fluorescence spectroscopy in the coastal upwelling system of the Ría de Vigo. *Marine Chemistry* 119: 121–129. https://doi.org/10.1016/j.marchem.2010.02.001.

Lu, Y., J.E. Bauer, E.A. Canuel, Y. Yamashita, R.M. Chambers, and R. Jaffé. 2013. Photochemical and microbial alteration of dissolved organic matter in temperate headwater streams associated with different land use. *Journal of Geophysical Research: Biogeosciences* 118: 566–580. https://doi.org/10.1002/jgrg.20048.

Martineac, R. P., A. V. Vorobev, M. A. Moran, and P. M. Medeiros. 2021. Assessing the contribution of seasonality, tides, and microbial processing to dissolved organic matter composition variability in a southeastern U.S. estuary. *Frontiers in Marine Science* 8: 781580. https://doi.org/10.3389/fmars.2021.781580.

McCallister, S., J. Bauer, J. Kelly, and H. Ducklow. 2005. Effects of sunlight on decomposition of estuarine dissolved organic C, N and P and bacterial metabolism. *Aquatic Microbial Ecology* 40: 25–35. https://doi.org/10.3354/ame040025.

McCallister, S., J.E. Bauer, and E.A. Canuel. 2006. Bioreactivity of estuarine dissolved organic matter: A combined geochemical and microbiological approach. *Limnology and Oceanography* 51: 94–100. https://doi.org/10.4319/lo.2006.51.1.0094.

McClain, M.E., E.W. Boyer, C.L. Dent, S.E. Gergel, N.B. Grimm, P.M. Groffman, S.C. Hart, et al. 2003. Biogeochemical hot spots and hot moments at the interface of terrestrial and aquatic ecosystems. *Ecosystems* 6: 301–312. https://doi.org/10.1007/s10021-003-0161-9.

Medeiros, P.M., M. Seidel, T. Dittmar, W.B. Whitman, and M.A. Moran. 2015. Drought-induced variability in dissolved organic matter composition in a marsh-dominated estuary. *Geophysical Research Letters* 42: 6446–6453. https://doi.org/10.1002/2015GL064653.

Medeiros, P. M., M. Seidel, S. M. Gifford, F. Ballantyne, T. Dittmar, W. B. Whitman, and M. A. Moran. 2017. Microbially-mediated transformations of estuarine dissolved organic matter. *Frontiers in Marine Science* 4: https://doi.org/10.3389/fmars.2017.00069.

Millard, S.P. 2013. *EnvStats: An R package for environmental statistics*. New York: Springer Science+Business Media.

Miller, W.L., and M.A. Moran. 1997. Interaction of photochemical and microbial processes in the degradation of refractory dissolved organic matter from a coastal marine environment. *Limnology*

and Oceanography 42: 1317–1324. https://doi.org/10.4319/lo.1997.42.6.1317.

Minor, E.C., M. Swenson, B.M. Mattson, and A.R. Oyler. 2014. Structural characterization of dissolved organic matter: A review of current techniques for isolation and analysis. *Environmental Science: Processes and Impacts* 16: 2064–2079. https://doi.org/10.1039/C4EM00062E.

Monsen, N.E., J.E. Cloern, and L.V. Lucas. 2002. A comment on the use of flushing time, residence time, and age as transport time scales. *Limnology and Oceanography* 47 (5): 1545–1553. https://doi.org/10.4319/lo.2002.47.5.1545.

Moran, M.A., W.M. Sheldon, and J.E. Sheldon. 1999. Biodegradation of riverine dissolved organic carbon in five estuaries of the southeastern United States. *Estuaries* 22: 55. https://doi.org/10.2307/1352927.

Moran, M.A., W.M. Sheldon, and R.G. Zepp. 2000. Carbon loss and optical property changes during long-term photochemical and biological degradation of estuarine dissolved organic matter. *Limnology and Oceanography* 45: 1254–1264. https://doi.org/10.4319/lo.2000.45.6.1254.

Mulholland, M. 2021. 2020 Virginia HABs: Estuarine monitoring summary. VA HAB Taskforce Meeting. Gloucester Point, VA. 15 June 2021. https://www.vdh.virginia.gov/content/uploads/sites/178/2021/01/Mulholland_2020-Estuarine-Blooms-Lower-Bay.pdf. Accessed 22 June 2023.

Murphy, K.R., C.A. Stedmon, D. Graeber, and R. Bro. 2013. Fluorescence spectroscopy and multi-way techniques. *PARAFAC. Analytical Methods* 5: 6557. https://doi.org/10.1039/c3ay41160e.

Najjar, Raymond G., C.R. Pyke, M.B. Adams, D. Breitburg, C. Hershner, M. Kemp, R. Howarth, et al. 2010. Potential climate-change impacts on the Chesapeake Bay. *Estuarine, Coastal and Shelf Science* 86: 1–20. https://doi.org/10.1016/j.ecss.2009.09.026.

Nelson, N.B., and D.A. Siegel. 2013. The Global distribution and dynamics of chromophoric dissolved organic matter. *Annual Review of Marine Science* 5: 447–476. https://doi.org/10.1146/annurev-marine-120710-100751.

Neubauer, S.C., and I.C. Anderson. 2003. Transport of dissolved inorganic carbon from a tidal freshwater marsh to the York River estuary. *Limnology and Oceanography* 48: 299–307. https://doi.org/10.4319/lo.2003.48.1.0299.

Officer, C.B. 1980. Box models revisited. In *Estuarine and wetland processes with emphasis on modeling*, ed. P. Hamilton and K.B. MacDonald, 65–114. New York: Plenum Press.

Osburn, C.L., L.T. Handsel, B.L. Peierls, and H.W. Paerl. 2016b. Predicting sources of dissolved organic nitrogen to an estuary from an Agro-Urban Coastal Watershed. *Environmental Science & Technology* 50: 8473–8484. https://doi.org/10.1021/acs.est.6b00053.

Osburn, C.L., J.N. Atar, T.J. Boyd, and M.T. Montgomery. 2019. Antecedent precipitation influences the bacterial processing of terrestrial dissolved organic matter in a North Carolina estuary. *Estuarine, Coastal and Shelf Science* 221: 119–131. https://doi.org/10.1016/j.ecss.2019.03.016.

Osburn, C. L., T. J. Boyd, M. T. Montgomery, T. S. Bianchi, R. B. Coffin, and H. W. Paerl. 2016a. Optical proxies for terrestrial dissolved organic matter in estuaries and coastal waters. *Frontiers in Marine Science 2*. https://doi.org/10.3389/fmars.2015.00127.

Pachiadaki, M.G., E. Sintes, K. Bergauer, J.M. Brown, N.R. Record, B.K. Swan, M.E. Mathyer, et al. 2017. Major role of nitrite-oxidizing bacteria in dark ocean carbon fixation. *Science* 358: 1046–1051. https://doi.org/10.1126/science.aan8260.

Petrone, K.C., J.S. Richards, and P.F. Grierson. 2009. Bioavailability and composition of dissolved organic carbon and nitrogen in a near coastal catchment of south-western Australia. *Biogeochemistry* 92: 27–40. https://doi.org/10.1007/s10533-008-9238-z.

Pisani, O., J.N. Boyer, D.C. Podgorski, C.R. Thomas, T. Coley, and R. Jaffé. 2017. Molecular composition and bioavailability of dissolved organic nitrogen in a lake flow-influenced river in south Florida, USA. *Aquatic Sciences* 79: 891–908. https://doi.org/10.1007/s00027-017-0540-5.

Pucher, M., U. Wünsch, G. Weigelhofer, K. Murphy, T. Hein, and D. Graeber. 2019. staRdom: Versatile software for analyzing spectroscopic data of dissolved organic matter in R. *Water* 11: 2366. https://doi.org/10.3390/w11112366.

Raymond, P.A., and J.E. Bauer. 2001. DOC cycling in a temperate estuary: A mass balance approach using natural ^{14}C and ^{13}C isotopes. *Limnology and Oceanography* 46: 655–667. https://doi.org/10.4319/lo.2001.46.3.0655.

Raymond, P.A., J.E. Bauer, and J.J. Cole. 2000. Atmospheric CO_2 evasion, dissolved inorganic carbon production, and net heterotrophy in the York River Estuary. *Limnology and Oceanography* 45: 1707–1717. https://doi.org/10.4319/lo.2000.45.8.1707.

Raymond, P.A., J.E. Saiers, and W.V. Sobczak. 2016. Hydrological and biogeochemical controls on watershed dissolved organic matter transport: Pulse-shunt concept. *Ecology* 97: 5–16. https://doi.org/10.1890/14-1684.1.

Reay, W.G. 2009. Water quality within the York River Estuary. *Journal of Coastal Research* 10057: 23–39. https://doi.org/10.2112/1551-5036-57.sp1.23.

Reay, W.G., and K.A. Moore. 2009. Introduction to the Chesapeake Bay National Estuarine Research Reserve in Virginia. *Journal of Coastal Research* 10057: 1–9. https://doi.org/10.2112/1551-5036-57.sp1.1.

Santos, L., A. Pinto, O. Filipe, Â. Cunha, E.B.H. Santos, and A. Almeida. 2016. Insights on the optical properties of estuarine DOM – Hydrological and biological influences. *PLoS ONE* 11: e0154519. https://doi.org/10.1371/journal.pone.0154519.

Schneider-Zapp, K., M.E. Salter, P.J. Mann, and R.C. Upstill-Goddard. 2013. Technical note: Comparison of storage strategies of sea surface microlayer samples. *Biogeosciences Discussions* 10 (2): 2835–2855. https://doi.org/10.5194/bgd-10-2835-2013.

Seitzinger, S.P., R.W. Sanders, and R. Styles. 2002. Bioavailability of DON from natural and anthropogenic sources to estuarine plankton. *Limnology and Oceanography* 47: 353–366. https://doi.org/10.4319/lo.2002.47.2.0353.

Sheer, H. 2012. Chlorophyll breakdown in aquatic ecosystems. *Proceedings of the National Academy of Sciences* 109: 17311–17312. https://doi/https://doi.org/10.1073/pnas.1214999109.

Sigleo, A.C., and S.A. Macko. 1985. Stable isotope and amino acid composition of estuarine dissolved colloidal material. In *Marine and estuarine geochemistry*, ed. A.C. Sigleo and A. Hattori, 29–46. Chelsea, Michigan: Lewis.

Sin, Y., R.L. Wetzel, and I.C. Anderson. 1999. Spatial and temporal characteristics of nutrient and phytoplankton dynamics in the York River Estuary, Virginia: Analyses of long-term data. *Estuaries* 22: 260. https://doi.org/10.2307/1352982.

Sipler, R.E. and D.A. Bronk. 2015. Dynamics of dissolved organic nitrogen. In: Biogeochemistry of Marine Dissolved Organic Matter. D.A. Hansell and C.A. Carlson (eds). pp 127–232. https://doi.org/10.1016/C2012-0-02714-7

Sleighter, R.L., and P.G. Hatcher. 2008. Molecular characterization of dissolved organic matter (DOM) along a river to ocean transect of the lower Chesapeake Bay by ultrahigh resolution electrospray ionization Fourier transform ion cyclotron resonance mass spectrometry. *Marine Chemistry* 110: 140–152. https://doi.org/10.1016/j.marchem.2008.04.008.

Smith, P., and Bogren, K. 2001. Determination of nitrate and/or nitrite in brackish or seawater by flow injection analysis colorimetry. QuikChem Method 31–107–04–1-E. Milwaukee: Lachat Instruments.

Smith, E., and R. Benner. 2005. Photochemical transformations of riverine dissolved organic matter: Effects on estuarine bacterial metabolism and nutrient demand. *Aquatic Microbial Ecology* 40: 37–50. https://doi.org/10.3354/ame040037.

Sobczak, W.V., J.E. Cloern, A.D. Jassby, and A.B. Müller-Solger. 2002. Bioavailability of organic matter in a highly disturbed estuary: The role of detrital and algal resources. *Proceedings of the National Academy of Sciences* 99: 8101–8105. https://doi.org/10.1073/pnas.122614399.

Spencer, R.G.M., J.M.E. Ahad, A. Baker, G.L. Cowie, R. Ganeshram, R.C. Upstill-Goddard, and G. Uher. 2007. The estuarine mixing behaviour of peatland derived dissolved organic carbon and its relationship to chromophoric dissolved organic matter in two North Sea estuaries (U.K.). *Estuarine, Coastal and Shelf Science* 74: 131–144. https://doi.org/10.1016/j.ecss.2007.03.032.

Spencer, R. G. M., G. R. Aiken, K. P. Wickland, R. G. Striegl, and P. J. Hernes. 2008. Seasonal and spatial variability in dissolved organic matter quantity and composition from the Yukon River basin, Alaska. *Global Biogeochemical Cycles* 22. https://doi.org/10.1029/2008GB003231.

Stanley, B. 2021. Differential nitrogen uptake by aquatic communities in a Chesapeake Bay tributary and in the coastal Alaskan Arctic. *Dissertations, Theses, and Masters Projects.* William & Mary. Paper 1673281827. https://doi.org/10.25773/v5-my8k-q838.

Stedmon, C. A., and N. B. Nelson. 2015. The optical properties of DOM in the ocean. In Biogeochemistry of Marine Dissolved Organic Matter, 481–508. Elsevier. https://doi.org/10.1016/B978-0-12-405940-5.00010-8.

Stubbins, A., J.-F. Lapierre, M. Berggren, Y.T. Prairie, T. Dittmar, and P.A. Del Giorgio. 2014. What's in an EEM? Molecular signatures associated with dissolved organic fluorescence in boreal Canada. *Environmental Science & Technology* 48: 10598–10606. https://doi.org/10.1021/es502086e.

Szymczak-Żyla, M., G. Kowalewska, and J.W. Louda. 2008. The influence of microorganisms on chlorophyll *a* degradation in the marine environment. *Limnology and Oceanography* 53: 851–862. https://doi.org/10.4319/lo.2008.53.2.0851.

Tzortziou, M., P.J. Neale, C.L. Osburn, J.P. Megonigal, N. Maie, and R. JaffÉ. 2008. Tidal marshes as a source of optically and chemically distinctive colored dissolved organic matter in the Chesapeake Bay. *Limnology and Oceanography* 53: 148–159. https://doi.org/10.4319/lo.2008.53.1.0148.

Vazquez, E., S. Amalfitano, S. Faz, and A. Butturini. 2011. Dissolved organic matter composition in a fragmented Mediterranean fluvial system under severe drought conditions. *Biogeochemistry* 102: 59–72. https://doi.org/10.1007/s10533-010-9421-x.

Voss, M., H.W. Bange, J.W. Dippner, J.J. Middelburg, J.P. Montoya, and B. Ward. 2013. The marine nitrogen cycle: Recent discoveries, uncertainties and the potential relevance of climate change. *Philosophical Transactions of the Royal Society of London. Series b, Biological Sciences* 368 (1621): 20130121. https://doi.org/10.1098/rstb.2013.0121.

Wiegner, T., and S. Seitzinger. 2001. Photochemical and microbial degradation of external dissolved organic matter inputs to rivers. *Aquatic Microbial Ecology* 24: 27–40. https://doi.org/10.3354/ame024027.

Wu, K., K. Lu, M. Dai, and Z. Liu. 2019. The bioavailability of riverine dissolved organic matter in coastal marine waters of southern Texas. *Estuarine, Coastal and Shelf Science* 231: 106477. https://doi.org/10.1016/j.ecss.2019.106477.

Wu, S., H. Hong, L. Qian, J. Xiong, Y. You, Z. Wu, J. Liu, J. Liu, C. Yan, and H. Lu. 2021. The fate of dissolved organic matter along the mangrove creek-to-estuary continuum. *Estuarine, Coastal and Shelf Science* 260: 107496. https://doi.org/10.1016/j.ecss.2021.107496.

Wymore, A.S., J. Potter, B. Rodríguez-Cardona, and W.H. McDowell. 2018. Using in-situ optical sensors to understand the biogeochemistry of dissolved organic matter across a stream network. *Water Resources Research* 54 (4): 2949–2958. https://doi.org/10.1002/2017WR022168.

Yao, X., R.E. Sipler, B.C. Stanley, Q.N. Roberts, M.P. Sanderson, C.B. Bott, and D.A. Bronk. 2019. Quantifying effluent dissolved organic nitrogen (EDON) uptake by microbial communities along a salinity gradient in the York River. *Estuaries and Coasts* 42: 1265–1280. https://doi.org/10.1007/s12237-019-00563-9.

Zark, M., and T. Dittmar. 2018. Universal molecular structures in natural dissolved organic matter. *Nature Communications* 9: 3178. https://doi.org/10.1038/s41467-018-05665-9.